CAPITAL UNIVERSITY OF SCIENCE AND TECHNOLOGY, ISLAMABAD

Equilibrium Solutions of Planar Restricted Rhomboidal Five-plus-Two Body Problems

by

Aneeta Fatima

A thesis submitted in partial fulfillment for the degree of Master of Philosophy

in the

Faculty of Computing
Department of Mathematics

2026

CERTIFICATE OF APPROVAL

Equilibrium Solutions of Planar Restricted Rhomboidal Five-plus-Two Body Problems

by

Aneeta Fatima

(MMT243003)

THESIS EXAMINING COMMITTEE

S. No.	Examiner	Name	Organization
(a)	External Examiner	Dr. Bushra Majeed	NUST, Islamabad
(b)	Internal Examiner	Dr. Rashid Ali	CUST, Islamabad

Dr. Abdul Rehman Kashif
Thesis Supervisor
September, 2026

Dr. Muhammad Sagheer
Head
Dept. of Mathematics
September, 2026

Dr. M. Abdul Qadir
Dean
Faculty of Computing
September, 2026

Author's Declaration

I, **Aneeta Fatima** hereby state that my MPhil thesis "**Equilibrium Solutions of Planar Restricted Rhomboidal Five-plus-Two Body Problems**" is my own work and has not been submitted previously by me for taking any degree from Capital University of Science and Technology, Islamabad or anywhere else in the country/abroad.

At any time if my statement is found to be incorrect even after my graduation, the University has the right to withdraw my MPhil Degree.

(Aneeta Fatima)

Registration No: MMT243003

Plagiarism Undertaking

I solemnly declare that research work presented in this thesis "**Equilibrium Solutions of Planar Restricted Rhomboidal Five-plus-Two Body Problems**" is solely my research work with no significant contribution from any other person. Small contribution/help wherever taken has been duly acknowledged and that complete thesis has been written by me.

I understand the zero tolerance policy of the HEC and Capital University of Science and Technology towards plagiarism. Therefore, I as an author of the above titled thesis declare that no portion of my thesis has been plagiarized and any material used as reference is properly referred/cited.

I undertake that if I am found guilty of any formal plagiarism in the above titled thesis even after award of MPhil Degree, the University reserves the right to withdraw/revoke my MPhil degree and that HEC and the University have the right to publish my name on the HEC/University website on which names of students are placed who submitted plagiarized work.

(Aneeta Fatima)

Registration No: MMT243003

Acknowledgement

All praise and gratitude to Almighty Allah, the Most Merciful, who blessed me with the strength, patience, and perseverance to complete this work. I am profoundly grateful to my supervisor, **Dr. Abdul Rehman Kashif**, for his invaluable guidance, constant encouragement, and scholarly insight throughout this research. His deep expertise in the N-body and restricted body problems shaped the direction of this thesis, and his patience and support made this journey possible. I extend my sincere thanks to **Dr. Muhammad Sagheer**, Head of the Department of Mathematics, and to the respected faculty members of the Department of Mathematics at the Capital University of Science and Technology (CUST), Islamabad — including **Dr. Rashid Ali**, **Dr. M. Sabeel Khan**, **Dr. Dur-e-Shehwar**, **Dr. Samina Batul**, and **Dr. Abid Kamran** — whose teaching, mentorship, and the stimulating academic environment they fostered laid the foundation of my mathematical understanding. The collaborative and research-driven culture at CUST has been a source of constant motivation.

Finally, I owe my deepest gratitude to my parents, my husband, and my brother, **Adnan Naseer**, for their unconditional love, prayers, and unwavering support, without which this accomplishment would not have been possible.

(Aneeta Fatima)

Registration No: MMT243003

Abstract

In this thesis, the equilibrium points of two mutually interacting test particles with masses m_1 and m_2 are determined under the gravitational influence of five primary masses, where $M_1 = M_2 = M_3 = M$ and $M_4 = M_5 = \tilde{M}$, in a uniformly rotating plane. We assume that $m_1, m_2 \ll M_i, i = 1, ..., 5$. The primary masses are expressed as functions of the distance parameters a and b, ensuring that they always form a rhomboidal central configuration within a specified range of these parameters. We derive the equations of motion for the two infinitesimal masses, which lead to a coupled system of nonlinear algebraic equations. In the case when $m_1 = m_2 = 0$, we recover twelve equilibrium points for an arbitrary secondary body (four located on the x-axis, four on the y-axis, and four off the coordinate axes). When the mutual gravitational interaction between the test masses is taken into account ($m_1 = m_2 = 10^{-6}$), each equilibrium point bifurcates into a symmetric pair whose center of mass coincides with the corresponding original equilibrium point. We also analyze the stability of equilibrium points and draw the possible regions of motion.

Contents

List of Figures

List of Tables

Abbreviations

2BP	Two-Body Problem
3BP	Three-Body Problem
5BP	Five-Body Problem
CC	Central Configuration
CoM	Center of Mass
CR3BP	Circular Restricted Three-Body Problem
NBP	N-Body Problem
R4BP	Restricted Four-Body Problem
R5BP	Restricted Five-Body Problem
RNBP	Restricted N-Body Problem
RR5BP	Restricted Rhomboidal Five-Body Problem
RR6BP	Restricted Rhomboidal Six-Body Problem
SI	International System of Units
ZVCs	Zero Velocity Curves

Symbols

Symbols	**Name**	**SI Units**
a	Acceleration	$\mathrm{m\,s^{-2}}$
F	Force	Newton (N)
F_c	Centrifugal force	Newton (N)
G	Universal gravitational constant	$\mathrm{N\,m^2\,kg^{-2}}$
g	Gravitational acceleration	$\mathrm{m\,s^{-2}}$
L	Angular momentum	$\mathrm{kg\,m^2\,s^{-1}}$
m	Mass of object	kilogram (kg)
p	Linear momentum	$\mathrm{kg\,m\,s^{-1}}$
r	Distance	meter (m)
W	Weight	Newton (N)
τ	Torque	Newton-meter (N m)
ω	Angular velocity	Radians per second (rad/s)
C	Jacobi Constant	
D_{2h}	Dihedral symmetry group	
e	Eccentricity of ellipse	
$f(r)$	Central force	
k	Scalar constant of proportionality	
L_i	Lagrange points	
λ	Eigenvalues	
$\tau(\mu)$	Mass ratio function	

Chapter 1

Introduction

In Celestial mechanics, we study the motion of celestial bodies including planets, moons, and comets and examine the effects of their mutual gravitational interactions. This field is founded on the principles of classical mechanics together with mathematical modeling to describe and predict orbital motion and trajectories in space. Among the most significant and longstanding challenges in celestial mechanics is the N-Body Problem (NBP), which focuses on determining the dynamical evolution of N mutually interacting bodies governed by Newton's law of universal gravitation. In general, no closed-form analytical solution exists for the NBP.

Sir Isaac Newton was first who addressed the case of Two-Body Problem (2BP) and successfully solved through the application of his universal law of gravitation. Newtonian mechanics, first introduced in his landmark work entitled "Philosophiae Naturalis Principia Mathematica" [1], provides the mathematical framework for describing gravitational motion. The 2BP serves as the fundamental basis for the analysis of multi-body dynamical systems, as it describes the motion of two point masses interacting exclusively through their mutual gravitational attraction. Kepler established that planets revolve around the Sun in elliptical orbits through his laws of planetary motion. Building upon these discoveries, Newton derived the mathematical formulation of Kepler's laws [2] and subsequently extended his investigations to more complex dynamical systems.

The dynamics become more complex when three or more bodies are involved. The general analytical solution of the Newtonian NBP does not exist because the governing equations become nonlinear and strongly coupled differential equations making a general closed-form solution unattainable. So, the researchers investigate special configurations and restricted versions of the $N-$bodies to gain insight into the dynamic behavior of the system [3]. Such studies are essential for understanding planetary systems in a multi-body environment. John.F.L Simmons et al. [4] explored how solar radiation pressure perturbs the orbits of dust, grains, and small bodies, expanding upon the classic Three-Body Problem (3BP).

In the RNBP, one or more infinitesimal masses move under the gravitational effect of massive primaries. The Circular Restricted Three-Body Problem (CR3BP) exhibit five equilibrium points where the test particle (like an asteroid or spacecraft) can stay fixed in the rotating frame due to the gravitational attraction of two much larger orbiting bodies (the Sun and Jupiter). Among the various special solutions of NBPs, Central Configuration has attracted considerable attention in recent years. Researchers have investigated it for planar and spatial $N-$body systems, symmetric configurations, equal-mass configurations, equilateral triangle and rhomboidal setups.

Extensions to four and five bodies with kite-shaped and rhomboidal central configurations have been classified and analyzed in detail. Symmetry reduction can be used to compute relative equilibria efficiently. These geometries are of great interest because they generate multiple families of equilibrium points when additional infinitesimal masses are introduced.

The RNBP is regraded as a key problem in celestial mechanics, even though a complete analytical solution has yet to be established. As a result, determining the number, location and stability of the equilibrium points of the restricted body remains a major focus of research in modern celestial mechanics. During the nineteenth century, extensive research on the NBP was undertaken by astronomers and mathematicians to better understand the equilibrium points that characterize multi-body gravitational systems. It has applications in astrodynamics (motion of Trojan asteroids, parking orbits for space telescopes, and defining low-energy pathways for interplanetary transport), spacecraft mission design, and the study of natural gravitational systems.

1.1 Historical Background and Literature Review

The present thesis is founded on the RNBP, which serves as a fundamental framework in celestial mechanics. The study of celestial mechanics originates from the law of universal gravitation yielding an exact analytical closed-form solution for the 2BP. However, for systems involving three or more bodies, no general analytical solution is available. The RNBP offers a practical simplification by assuming that one or more bodies possess negligible mass, allowing their gravitational influence on the massive primary bodies to be neglected while their own motion remains governed by the gravitational effect of primaries.

The general problem of three bodies was introduced by Leonhard Euler in 1767. He discovered three collinear solutions in which the bodies aligned in a straight line [5]. After five years, Lagrange extended Euler's results by finding two additional solutions forming an equilateral triangle that rotates rigidly [6]. These five solutions are called Lagrange points. These points are important positions for satellites, communication systems and observatories and became the core of the CR3BP.

The mathematical nature of the problem changed when Henri Poincaré [7] in 1892 proved that the general solution of three bodies is non-integrable. His proof forced researchers to focus on restricted models. The CR3BP was formalized in the 20$^{\text{th}}$ century, where two massive primaries move in circular orbits and a third test particle has negligible mass. In 1967, Szebehely et al. [8] provided the definitive treatment by introducing the rotating synodic frame, the effective potential and the Jacobi integral. His book became the standard reference for CR3BP theory and application. Arthur L. Whipple [9] in 1984 was the first to move beyond three bodies by studying the restricted $2 + 2$ problem. He replaced one primary of the

Circular CR3BP with a binary pair and placed two test masses in the system, mutually attracting each other but not perturbing the primaries. Whipple showed that each Lagrange point of the CR3BP splits into two equilibrium points because the symmetry of the system is broken. His work introduced the $n + k$ notation and found that the number of equilibrium points increases with an increase in the number of primaries.

Between 1910 and 1930, Moulton [10] classified Central Configuration for $N \leq 4$ that allows periodic or rotating solutions and is important for restricted problems. Later on, the special geometric arrangements of primaries have been widely explored because symmetry simplifies the governing equations. Among these arrangements, the rhomboidal configurations are of particular importance. In this configuration, the primaries form vertices of a rhombus while rotating uniformly around their center of mass. Kulesza et al. [11] examined an RR5BP and applied both analytical techniques and numerical simulations to determine the equilibrium points and map out the regions of possible central configuration. Albouy and Vadim [12] made huge contributions to the NBP, particularly regarding the classification and symmetry of Central Configuration.

Alexander Ollongren [13] investigated a restricted five-body configuration, where three bodies of equal mass were placed at the corners of a uniformly rotating equilateral triangle, while fourth primary with a larger mass was situated at the centroid of triangle. An additional body of negligible mass was considered to move within the same plane under the gravitational influence of the primary bodies. By employing computer-assisted analytical techniques, he systematically examined the dynamical characteristics of this configuration.

Papadakis and Kanavos [14] examined the restricted photogravitational 5BP by analyzing the motion of an infinitesimal particle on a sphere. Their study considered four primary bodies located at the vertices of a square together with a test particle moving under their combined gravitational field. Using numerical continuation methods, they identified sixteen equilibrium points and investigated their corresponding stability regions. This work established an important foundation for the study of higher-order restricted problems involving specific geometric arrangements of the primary bodies. Likewise, Gidea and Jaume Llibre [15] made significant contributions to the analysis of geometric and symmetric configurations in gravitational dynamical systems. Their investigations of invariant manifolds and equilibrium points have provided valuable insights for the design of low-energy spacecraft trajectories. Lee and Santoprete [16] investigated the symmetry properties of the equilibrium points associated with the R5BP. Furthermore, Palmore [17] established several fundamental theorems concerning equilibrium points in the planar NBP. He demonstrated that, for any prescribed set of masses and configurations, the number of relative equilibrium solutions is always finite.

A new geometric configuration for five bodies was discovered by Shoaib et al. [18] in 2017. They proved that five bodies can form a stable rotating rhombus with one body at the center. They also found that, unlike the equilateral triangle and square, the rhombus is non-axisymmetric, making it a most general case for the restricted problem. Jagadish and Aguda [19] worked on the Restricted Four-Body Problem (R4BP) and evaluated how gravitational forces and radiation pressure affect the stability and movement of a test particle orbiting three larger primary masses.

Corbera et al. [20] showed that any convex central configuration of four bodies with orthogonal diagonals leads to a kite geometry. Their result was proven for both the general power-law potential and the planar vortex system. Lara and Bengochea [21] performed both theoretical and numerical studies of symmetric periodic trajectories in the four-body problem by making the use of time-reversal symmetries. Alsaedi et al. [22] employed computational algorithms together with variational techniques to identify collision-free periodic orbits exhibiting regular repeating patterns in the six-body problem. Javaid Idrisi and Shahzaib Ullah[23] investigated the central configurations (CC) and the stability of equilibrium points of restricted six body system. Their analysis revealed that all equilibrium points are distributed on three concentric circles centered at the origin. Euaggelos E. Zotos [24] carried out numerical work on the linearly stable equilibrium points of the restricted problem of four bodies where primary bodies arranged in a triangular configuration. In addition, he used computational basin analysis to the CR3BP and applied the Newton–Raphson iterative scheme to determine the convergence of each each Lagrange point [25].

In 2021, Siddique et al. [26] analyzed the stability of equilibrium points for the Rhomboidal Restricted problem of Six bodies. In this model, four primary masses are forming a shape of rhombus and the fifth mass is placed at the intersection point of its diagonals. These five primary bodies continuously maintain a rhomboidal central configuration (CC), whereas the sixth body is treated as infinitesimal compared to the others.

To remove the explicit time dependence from the equations of motion, they formulated the problem in a rotating frame. The authors further investigated the Hill regions and the admissible domains of motion for the test particle using the Jacobi constant along with the effective potential. Their analysis identified a total of twelve equilibrium points, including four located at x-axis, other four lie at the y-axis and four lying off the coordinate axes. They also noted that the positions of these equilibrium points vary with changes in the mass parameters of the system. Furthermore, a linear stability analysis indicated that all of equilibrium points are unstable.

1.2 Research Gap and Thesis Contribution

Research on the NBP progressed from Newton's solution of 2BP to the study of Lagrange points, and then from the solution of the CR3BP to the restricted problems of four an five bodies with special geometrical arrangements. The present study is an extension of the Rhomboidal Restricted Six-Body Problem (RR6BP) by Siddique et al. [26], since the $5+2$ problem has not been analyzed for rhombus symmetry.

In this study, two infinitesimal test particles are considered moving under the gravitational field produced by five primary bodies arranged in a rhomboidal central configuration. The corresponding equations of motion are formulated by including the mutual gravitational interaction between the two infinitesimal bodies. Furthermore, the effects of the mass and geometric parameters on the existence and distribution of the equilibrium points are investigated, along with their symmetry properties and linear stability.

Numerical computations are performed using the formulation introduced by Whipple [9] for the restricted $2+2$ body problem, where two bodies were assumed to have negligible-mass. The proposed model extends the classical Lagrange equilibrium points (L_4, L_5) and Euler equilibrium points (L_1, L_2, L_3) to a rhomboidal configuration containing two mutually interacting test particles, thereby establishing a connection between the integrable circular restricted three-body problems and the more general dynamics of the N-body system.

1.3 Dissertation Outline

Our research on the rhomboidal $5+2$ body problems is structured as follows:

In **Chapter 1**, introduction and historical background of the RNBP and relevant literature are provided and also observe the research gap and significance of the study.

In **Chapter 2** there are some basic concepts of dynamical systems and key terms related to celestial mechanics both theoretically and mathematically.

In **Chapter 3** the geometry of the system, mass distribution of primaries and conditions for the CC of rhomboidal primary masses are determined and also discuss three cases where the condition of CC is satisfied, and mention two extreme cases for which the CC of the problem degenerates. Finally, calculate the equilibrium points numerially for two secondary masses.

In **Chapter 4** the equations of motion for two secondary bodies are formulated and find equilibrium points numerically by using the effective potential function together with the formulae proposed by Whipple. Furthermore, the physical significance of obtained results, symmetry and stability of equilibrium solutions, and admissible regions of motion for test particles are discussed.

In **Chapter 5** the major findings of the present study are summarized with applications and concluding remarks.

In the **Bibliography** all the references used in the thesis are mentioned.

Chapter 2

Preliminaries

This chapter introduces the core concepts, basic definitions and principles of classical mechanics, and the governing laws that constitute the theoretical framework required for understanding the analyses and results presented in the next chapters.

2.1 Basic Definitions

2.1.1 Motion

Motion is the continuous change in the state of an object or body over time relative to a reference point. Depending on its path, motion may be linear, rotational, vibratory, or periodic [27].

2.1.2 Mechanics

This is the branch of physics concerned with the study of the motion of objects along with the forces acting upon them. Mechanics is further divided into kinematics (geometry) and dynamics (causes) of motion. [27].

It depends on laws of motion and gravitation. Mechanics is used everywhere from planets orbiting the Sun to designing the machines and bridges.

2.1.3 Force

In physics, an interaction that changes the state of motion of an object is known as force. Force is vector quantity characterized by the magnitude as well as direction. In everyday terms, force is a push or pull. It is expressed through Newton's second law of motion as,

$$\mathbf{F} = m\mathbf{a}, \tag{2.1}$$

where m represents the mass of an object and a stands for acceleration [27].

2.1.4 Torque

Torque [27] is a rotational force expresses as,

$$\boldsymbol{\tau} = \mathbf{r} \times \mathbf{F},$$

Here $\boldsymbol{r}$ is the position vector of the object in a force field $\mathbf{F}$ relative to the pivot point O. The unit of torque is the newton meter (N m). The magnitude of $\boldsymbol{\tau}$ is given by,

$$\boldsymbol{\tau} = rF\sin\theta.$$

2.1.5 Momentum

The linear momentum [27] of a particle is the product of its mass and velocity and is represented by $\boldsymbol{p}$. Newton's second law of motion can be reformulated using momentum, so that the rate of change of the linear momentum is equal to the net external force acting on the object.

$$\sum \boldsymbol{F} = m\boldsymbol{a} = m\,\frac{d\boldsymbol{v}}{dt} = \frac{d(m\boldsymbol{v})}{dt} = \frac{d\boldsymbol{p}}{dt}.$$

Momentum plays a vital role in understanding the motion of celestial bodies like stars, moons, planets, comets, galaxies and spacecraft during gravitational interactions. It is also used in rocket propulsion, sports and collisions.

2.1.6 Central Force

A physical force acting on an object of mass m is termed as central force if it is always directed from m towards or away from a fixed point O. The magnitude of this force is a function of the distance r between the object and the center O. Mathematically, the central force is represented as

$$\mathbf{F} = f(r)\,\mathbf{r_1}, \tag{2.2}$$

where $\mathbf{r_1}$ is the unit vector in the direction of distance $\mathbf{r}$. This force is one of attraction towards O it $f(r) < 0$ and repulsion from O if $f(r) > 0$ [27].

2.1.7 Center of Mass

It is a unique point in a system of objects where the total mass can be assumed to be concentrated. It serves as a balance point for the entire body. Suppose we have a system of n masses $m_1, m_2, \ldots, m_n$ with their position vectors, $\mathbf{r}_1, \mathbf{r}_2, \ldots, \mathbf{r}_n$ respectively; then the center of mass of the system is defined as the point having the position vector

$$\mathbf{R}_{CoM} = \frac{1}{M}\sum_{i=1}^{n} m_i\mathbf{r}_i, \qquad \text{where } M = \sum_{i=1}^{n} m_i. \tag{2.3}$$

The center of mass (CoM) is also known as centroid [27].

2.1.8 Center of Gravity

Center of gravity [27] is an imaginary point in an object where the whole weight of the body is concentrated. It can also be defined as the weighted average position of the gravitational forces acting on each mass element.

$$\mathbf{R}_{CG} = \frac{\sum_{i=1}^{n} W_i\mathbf{r}_i}{\sum_{i=1}^{n} W_i}, \qquad \text{where } W = mg. \tag{2.4}$$

2.1.9 Field

A field is a physical quantity is defined at every point in space and time. This quantity can be in scalar, vector, or tensor form. Field explains how masses or objects interact through the space between them [27].

2.1.10 Gravitational Field

A gravitational field is an invisible force field, a region of space surrounding any massive body in which another mass experiences a gravitational effect. The intensity of this field is known as the gravitational field strength, denoted by g. Mathematically,

$$g = \frac{\mathbf{F}}{m}, \tag{2.5}$$

where $\mathbf{F}$ is the gravitational force exerted on an object per unit mass m. It is also expressed as

$$g = G\frac{M}{r^2} \tag{2.6}$$

when a specific mass produces a gravitational field. It is measured in meters per second squared or newtons per kilogram [27].

2.1.11 Potential Energy

It is the stored energy of an object or system due to its state, position and configuration relative to other objects. Potential energy is not a physical substance but a property of a system of interacting objects governed by conservative forces like gravity or electromagnetism [27].

2.1.12 Newton's Universal Law of Gravitation

This law states that any two particles in the universe exerts an attractive force on each other which is directly proportional to the product of their masses and inversely proportional to the square of the distance between them. This is represented as

$$\mathbf{F} = G\frac{m_1 m_2}{r^2}, \tag{2.7}$$

Here G is gravitational constant with the approximate value $6.67 \times 10^{-11}\ \mathrm{N\,m^2\,kg^{-2}}$ [27].

2.1.13 Kepler's Laws of Planetary Motion

Kepler proposed the following foundational laws of astronomy that explain how planets orbit the Sun.

(i) All the planets move around the Sun in an elliptical orbit with the Sun at one focus.

(ii) A line joining the center of the Sun to the center of a planet covers equal areas in equal durations.

(iii) The square of the revolution period of a planet is proportional to the cube of the semi-major axis a of its elliptical orbit [27].

2.1.14 Newton's Laws of Motion

(i) Every object maintains the state of rest or uniform linear motion unless it is compelled to change that state by an external force acting upon it [27].

(ii) When a force acts on a body, it produces acceleration. The acceleration is directly proportional to the applied force and inversely proportional to the mass. This is expressed as,

$$\mathbf{F} = m\mathbf{a}. \tag{2.8}$$

(iii) For every action, there is an equal and opposite reaction. We are able to walk and push or pull the objects because of this law. Planets and moons attract each other through gravitational force and keep orbits stable.

2.1.15 Inertial Frame of Reference

An inertial frame of reference is a coordinate system that is either stationary or moving with uniform velocity with respect to other frames of reference. Within such a frame, object remains at rest or continues moving in a straight line at constant speed unless acted upon by an external force, leading to zero acceleration. Newton's laws of motion hold are valid in all inertial frames of reference. A frame where Newton's laws are invalid is called a non-inertial frame of reference [27].

2.2 Celestial Mechanics

Celestial mechanics deals with the calculation and prediction of the motion, gravitational interaction and trajectories of objects in outer space. It is the oldest branch of astronomy, founded by Newton. Classical mechanics provides the foundation for this field through the universal law of gravitation and Newton's laws of motion, and Kepler's laws of planetary motion to analyze the motion of moons, stars and planets. Newtonian mechanics produces a set of orbital elements that can predict the future location of two bodies with reasonable accuracy, but a complication arises when a third body is added. In this case, perturbation theory finds an approximate solution of the problem. It has real-world applications in Earth sciences, celestial navigation, space exploration, satellite operations, etc [27].

2.2.1 Angular Velocity

The rate at which an object rotates around a specific center or axis is referred as angular velocity. It is represented by the symbol ω and calculated by the formula,

$$\omega = \frac{\Delta\theta}{\Delta t}. \tag{2.9}$$

Radians per second is its standard unit in physics [27]. The angular velocity of the planets increases when they are closer to the Sun and decreases when farther.

2.2.2 Centrifugal Force

Centrifugal force [28] is an apparent or fictitious force experienced by an object in a rotating frame. It acts radially outward from the CoM. It is not an actual push or pull but rather a consequence of inertia. Consider an object of mass m moving in a circular path of radius r with angular velocity ω. The centrifugal force is calculated by the formula

$$\mathbf{F}_c = mr\omega^2. \tag{2.10}$$

2.2.3 Rotating or Synodic Coordinate System

It is a non-inertial reference frame that revolves around a central mass with constant angular velocity. It is called ‘"synodic" because the frame period matches the orbital period of the primaries. It is useful when calculating the Lagrange points [29].

2.2.4 Infinitesimal Mass or Test Particle

In celestial mechanics, a test particle is an object with negligible mass so that it cannot exert any gravitational influence or back-reaction on the larger bodies in return for their gravitational pull. By treating one of the objects as having negligible mass, physicists simplify complex calculations [29].

2.2.5 Lagrange Points

Lagrange points are particular locations in space where a test particle under the gravitational influence of two large masses can stay fixed relative to the larger ones. Spacecraft use these parking spots to maintain their position. Lagrange was a French astronomer and mathematician who found these points for the Sun-Earth system. Lagrange points are also referred to as equilibrium or libration points [27].

2.2.6 Equilibrium Solutions

An equilibrium point is a state in a system where all variables or opposing forces are perfectly balanced, resulting in no net change over time. These solutions can be found only if we meet the sufficient condition, i.e., all rates are equal to zero. In the case of two variables,

$$\dot{x} = \dot{y} = \ddot{x} = \ddot{y} = \ldots = x^{(n)} = y^{(n)} = 0. \tag{2.11}$$

Equilibrium solutions may be stable or unstable. [27]."

2.2.7 Linear Stability of Equilibrium Solutions

Linear stability analyzes whether a small disturbance or perturbation to an equilibrium point of a system decays, grows or remains bounded over time. The decay of perturbations indicates stability, i.e., the object stays bound to the region; if they grow, the point is unstable. The stability of solutions depends on the differential equations and the potential energy [27]. To check the stability, we add a small disturbance to the original equilibrium point and substitute it into the system of equations and linearize the system about the equilibrium point by taking only the first term.

2.3 Solution of Two-Body Problem

This problem describes the motion of a body subjected to the gravitational attraction of another body. It is the foundation for orbital mechanics and solving more complex problems of N-bodies in celestial mechanics. Consider two masses, m_1 and m_2, interacting through their mutual gravitational force. The force $\mathbf{F}_1$ acting on the mass m_1 is directed toward m_2 along the position vector $\mathbf{r}$, whereas the force $\mathbf{F}_2$ acting on m_2 has the same magnitude but opposite in direction, as illustrated in Figure 2.1.

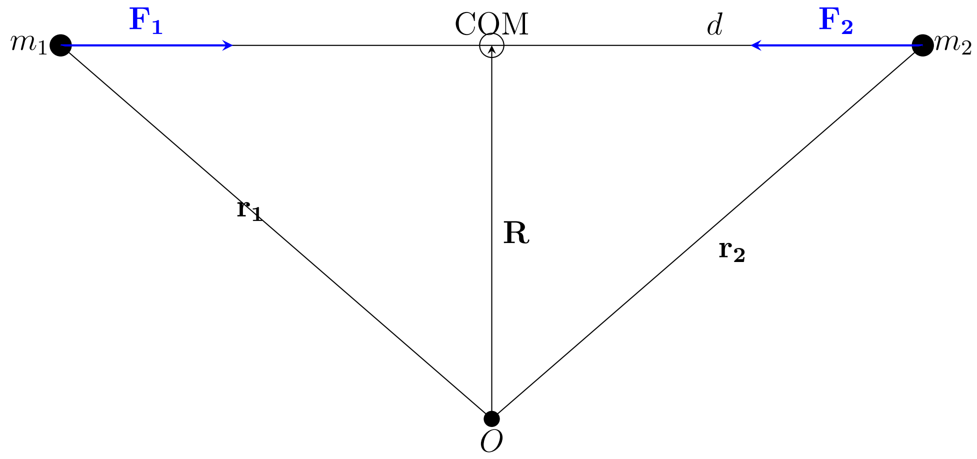

Figure 2.1: Geometry of the two-body problem: the masses m_1 and m_2 with position vectors $\mathbf{r_1}$ and $\mathbf{r_2}$ measured from the origin O, the centre of mass (COM) located at $\mathbf{R}$, and the mutually attractive gravitational forces $\mathbf{F_1}$ and $\mathbf{F_2}$.

By Newton's third law,

$$\mathbf{F_1} = -\mathbf{F_2}, \tag{2.12}$$

where

$$\mathbf{F_1} = G\,\frac{m_1 m_2}{r^3}\,\mathbf{r}. \tag{2.13}$$

By applying Newton's second law of motion in conjunction with the above equations 2.12 and 2.13, we obtain

$$m_1\ddot{\mathbf{r}}_1 = G\,\frac{m_1 m_2}{r^3}\,\mathbf{r}, \tag{2.14}$$

$$m_2\ddot{\mathbf{r}} = -G\,\frac{m_1 m_2}{r^3}\,\mathbf{r}. \tag{2.15}$$

Now, adding equations 2.14 and 2.15 we get,

$$m_1\ddot{\mathbf{r_1}} + m_2\ddot{\mathbf{r}}_2 = 0. \tag{2.16}$$

Upon performing the integration of equation 2.16 with respect to time we arrive at the conclusion that the weighted sum of position vectors of two masses remains constant. Consequently we obtain the following,

$$m_1\dot{\mathbf{r}}_1 + m_2\dot{\mathbf{r}}_2 = k_1. \tag{2.17}$$

The integration of the above equation yields,

$$m_1\mathbf{r_1} + m_2\mathbf{r_2} = k_1 t + k_2, \tag{2.18}$$

where k_1 and k_2 are constants of integration. The center of mass $\mathbf{R}$ is defined as

$$\mathbf{R} = \frac{m_1\mathbf{r_1} + m_2\mathbf{r_2}}{m_1 + m_2},$$

$$(m_1 + m_2)\,\mathbf{R} = m_1\mathbf{r_1} + m_2\mathbf{r_2},$$

$$m_t\,\mathbf{R} = m_1\mathbf{r_1} + m_2\mathbf{r_2}, \tag{2.19}$$

where $m_1 + m_2 = m_t$. Now, using equation 2.19 in equation 2.18 we get

$$m_t\,\mathbf{R} = k_1 t + k_2.$$

Differentiation of above equation implies,

$$\dot{\mathbf{R}} = \frac{k_1}{m_t} = \text{constant}.$$

This follows that the center of mas o system moves with a uniform velocity. Now, subtracting equation 2.15 from equation 2.14 gives

$$\ddot{\mathbf{r}}_1 - \ddot{\mathbf{r}}_2 = G\,(m_1 + m_2)\,\frac{\mathbf{r}}{r^3},$$

$$\ddot{\mathbf{r}} = \alpha\,\frac{\mathbf{r}}{r^3},$$

where we set $G(m_1 + m_2) = \alpha$ and $\mathbf{r} = \mathbf{r_1} - \mathbf{r_2}$. Rearranging this we obtain the fundamental differential equation of the Two-body problem.

$$\ddot{\mathbf{r}} - \alpha\,\frac{\mathbf{r}}{r^3} = 0. \tag{2.20}$$

Taking the cross product $\mathbf{r}$ with equation 2.20, we obtain

$$\mathbf{r} \times \ddot{\mathbf{r}} - \alpha\,\frac{\mathbf{r}}{\mathbf{r^3}} \times \mathbf{r} = \mathbf{0}.$$

Since the cross product of any vector with itself is zero. Hence $\mathbf{r} \times \mathbf{r} = \mathbf{0}$. This leads to the expression,

$$\mathbf{r} \times \ddot{\mathbf{r}} = \mathbf{0}. \tag{2.21}$$

By integrating the above equation we obtain,

$$\mathbf{r} \times \dot{\mathbf{r}} = \mathbf{L},$$

where $\mathbf{L}$ is an integration constant, which is the angular momentum here. We can write equation 2.21 as

$$\mathbf{r} \times \alpha\ddot{\mathbf{r}} = \mathbf{0},$$

$$\mathbf{r} \times \mathbf{F} = 0, \tag{2.22}$$

where we assumed $\mathbf{F} = \alpha\ddot{\vec{r}}$. As we know that the rate of change of angular momentum is equal to the torque acting on a system, using equation 2.22 the result is

$$\tau = \frac{d\mathbf{L}}{dt} = \mathbf{r} \times \mathbf{F} = 0,$$

$$\frac{d\mathbf{L}}{dt} = 0.$$

Upon integration we obtain,

$$\mathbf{L} = \text{constant}.$$

This result demonstrates that the angular momentum for the two-body system is conserved. [30].

2.4 Restricted N-Body Problem

The restricted -body problem is a simplified version of general N-body problem. In such problems, there are $N - 1$ massive primary bodies and one test particle that moves under their gravitational influence without affecting the large bodies in return. The focus is reduced to solving the kinematics and orbit of the single massless particle. The equation governing the motion of test particle is,

$$\ddot{\mathbf{r}} = G\sum_{i=1}^{N-1}\frac{m_i(\mathbf{r}_i-\mathbf{r})}{|\mathbf{r}_i-\mathbf{r}|^3}, \tag{2.23}$$

where $\ddot{\mathbf{r}}$ is the acceleration of the test particle having position vector $\mathbf{r}$ and m_i denotes the mass of primary body with position vector $\mathbf{r}_i$ [31].

2.4.1 Effective Potential

An effective potential [29] is a single function that contains multiple opposing physical effects (like the true potential energy and the centrifugal force). For the synodic rotating coordinates x and y, the motion of test particle is governed by the following equations,

$$\ddot{x} - 2\dot{y} = T_x, \tag{2.24}$$

$$\ddot{y} + 2\dot{x} = T_y, \tag{2.25}$$

where T is the effective potential defined as

$$T = G\sum_{i=1}^{N-1}\frac{m_i}{r_i} + \frac{1}{2}\left(x^2+y^2\right), \qquad r_i = \sqrt{(x-x_i)^2+(y-y_i)^2}. \tag{2.26}$$

2.4.2 Hill Regions and Zero-Velocity Curves

Hill regions are the specific zones of permitted motion for small object under the gravitational influence of larger bodies. These regions indicate the allowed and restricted space of motion. In a rotating coordinate system, the total energy of an infinitesimal mass is defined by a mathematical value known as the Jacobi constant, represented by the equation $v^2 = 2U - C$ where v denotes the velocity of restricted secondary body. Zero velocity curves (ZVCs) act as constraints preventing any small object moving under the gravitational pull of larger bodies from crossing them. These surfaces are determined by $2U - C = 0$. C is the constant of motion for the secondary bodies same to the energy and angular momentum in

2BP. The permissible motion regions for test particle are identified by $2U - C > 0$ to prevent negative values for v^2 [32].

2.5 Circular Restricted Three-Body Problem

In this model, two primary bodies with masses $\left(m_1 = 1-\mu,\ m_2 = \mu,\ \text{where } \mu \leq \frac{1}{2}\right)$ move in a circular orbit about their shared center of mass while exerting gravitational attraction on a third body whose mass is assumed negligible. The trajectories of the two primary bodies, m_1 and m_2, are considered to be known in advance, whereas the main objective is to study the motion of the third body (m_3). For simplicity, the gravitational constant G is normalized to unity [32].

Consider a cartesian coordinate system (ξ, η, ζ), established in an inertial reference frame, whose origin is placed at the center of mass of the two primary bodies, m_1 and m_2. The orbital plane of the primaries is assumed to coincide with the ξ–η plane, and at the initial instant $(t = 0)$, both bodies are positioned on the ξ-axis.

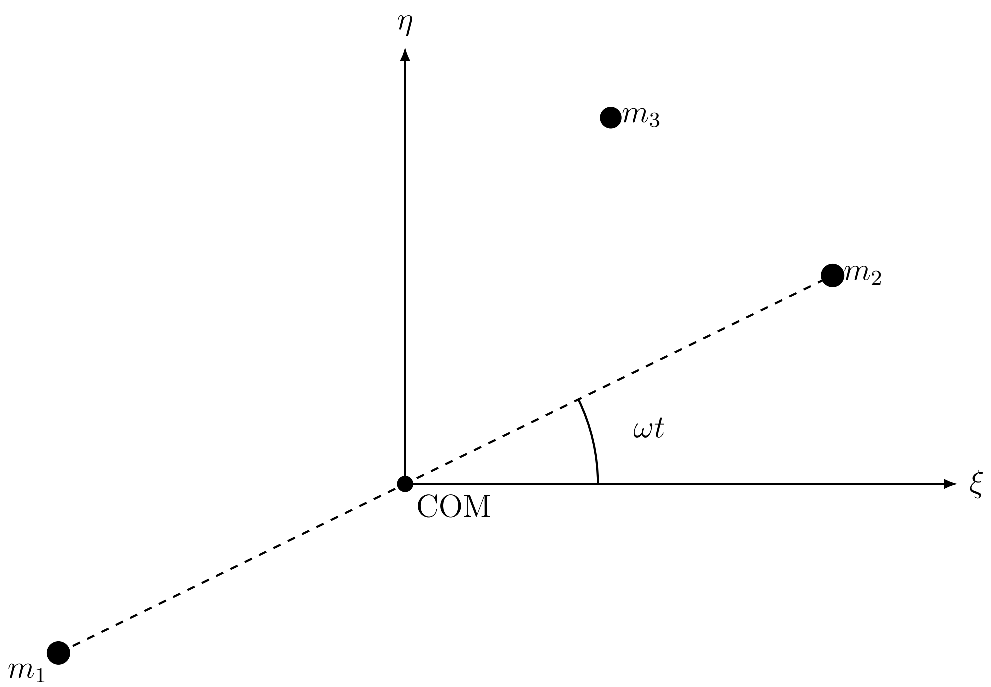

Figure 2.2: Restricted Three-Body Problem

If the positions of m_1 and m_2 are given by (ξ_1, η_1, ζ_1) and (ξ_2, η_2, ζ_2) with respect to the inertial axes (ξ, η, ζ), then the equation of motion of the third particle is:

$$\ddot{\boldsymbol{r}}_3 = \sum_{\substack{j=1 \\ j\neq 3}}^{3} m_j \frac{(\boldsymbol{r}_3 - \boldsymbol{r}_j)}{|\boldsymbol{r}_3 - \boldsymbol{r}_j|^3}$$

$$\Rightarrow \quad \begin{bmatrix} \ddot{\xi} \\ \ddot{\eta} \\ \ddot{\zeta} \end{bmatrix} = \frac{1-\mu}{r_1^3} \begin{bmatrix} \xi_1 - \xi \\ \eta_1 - \eta \\ \zeta_1 - \zeta \end{bmatrix} + \frac{\mu}{r_2^3} \begin{bmatrix} \xi_2 - \xi \\ \eta_2 - \eta \\ \zeta_2 - \zeta \end{bmatrix} \tag{2.27}$$

where,

$$r_1^3 = |\boldsymbol{r}_3 - \boldsymbol{r}_1|^3 = \left[(\xi_1 - \xi)^2 + (\eta_1 - \eta)^2 + (\zeta_1 - \zeta)^2\right]^{3/2},$$

and

$$r_2^3 = |\boldsymbol{r}_3 - \boldsymbol{r}_2|^3 = \left[(\xi_2 - \xi)^2 + (\eta_2 - \eta)^2 + (\zeta_2 - \zeta)^2\right]^{3/2}. \tag{2.28}$$

If the ζ-axis is perpendicular to the orbital plane of two massive primary bodies (with coordinates (x, y, z)), then $\zeta_1 = \zeta_2 = 0$ and $\zeta = z$.

The orientation of the x-axis can be selected such that m_1 and m_2 always lie on it with coordinates $(x_1, 0, 0)$ and $(x_2, 0, 0)$ respectively.

Hence,

$$\begin{aligned} r_1^3 &= \left[(x_1 - x)^2 + y^2 + z^2\right]^{3/2}, \\ r_2^3 &= \left[(x_2 - x)^2 + y^2 + z^2\right]^{3/2}. \end{aligned} \tag{2.29}$$

where (x, y, z) the coordinates are m_3 w.r.t. the rotating axes.

In the rotating frame, using the rotational matrix we get:

$$\left.\begin{aligned} \xi &= x\cos t - y\sin t, \\ \eta &= x\sin t + y\cos t, \\ \zeta &= z. \end{aligned}\right\} \tag{2.30}$$

Similarly,

$$\left.\begin{aligned} \xi_1 &= x_1 \cos t, & \xi_2 &= x_2 \cos t, \\ \eta_1 &= x_1 \sin t, & \eta_2 &= x_2 \sin t, \\ \zeta_1 &= 0, & \zeta_2 &= 0. \end{aligned}\right\} \tag{2.31}$$

By Using 2.30 and 2.31 in 2.27 and after simplification,we obtain the equations of motion of test particle in component form as follows,

$$\left.\begin{aligned} \ddot{x} - 2\dot{y} &= x - \frac{1-\mu}{r_1^3}(x - x_1) - \frac{\mu}{r_2^3}(x - x_2), \\ \ddot{y} + 2\dot{x} &= y - \left(\frac{1-\mu}{r_1^3} + \frac{\mu}{r_2^3}\right) y, \\ \ddot{z} &= -\left(\frac{1-\mu}{r_1^3} + \frac{\mu}{r_2^3}\right) z. \end{aligned}\right\} \tag{2.32}$$

We are not interested in the solution of these differential equations. We will just find the equilibrium points of test mass. So for the equilibrium points, set them $\dot{x} = \dot{y} = \dot{z} = \ddot{x} = \ddot{y} = \ddot{z} = 0$ in equation 2.32. The new equations are now:

$$\left.\begin{aligned} x &= \frac{1-\mu}{r_1^3}(x - x_1) + \frac{\mu}{r_2^3}(x - x_2) \\ y &= \left(\frac{1-\mu}{r_1^3} + \frac{\mu}{r_2^3}\right) y \\ 0 &= -\left(\frac{1-\mu}{r_1^3} + \frac{\mu}{r_2^3}\right) z \end{aligned}\right\} \tag{2.33}$$

Since $\left(\frac{1-\mu}{r_1^3} + \frac{\mu}{r_2^3}\right) \neq 0$, hence $z = 0$.

Now suppose, for $y \neq 0$, we get

$$\frac{1-\mu}{r_1^3} + \frac{\mu}{r_2^3} = 1 \;\Rightarrow\; \frac{1-\mu}{r_1^3} = 1 - \frac{\mu}{r_2^3}. \tag{2.34}$$

Making use of the above equation in 2.33, after simplification we get,

$$x_1 = \frac{\mu}{r_2^3}(x_1 - x_2) \;\Rightarrow\; x_1 = \frac{-x_1}{r_2^3}(-1) \;\Rightarrow\; r_2 = 1. \tag{2.35}$$

Now 2.34 gives ,

$$\frac{1-\mu}{r_1^3} + \frac{\mu}{1} = 1 \;\Rightarrow\; \frac{1-\mu}{r_1^3} = 1-\mu \;\Rightarrow\; r_1 = 1. \tag{2.36}$$

So equations 2.29 becomes,

$$\left.\begin{aligned} 1 &= (x_1 - x)^2 + y^2, \\ 1 &= (x_2 - x)^2 + y^2. \end{aligned}\right\} \tag{2.37}$$

Subtraction and simplification of both above equations return,

$$x = \frac{x_1 + x_2}{2}. \tag{2.38}$$

Using the value of x in one of the equations 2.37 we get,

$$y = \pm\frac{\sqrt{3}}{2}. \tag{2.39}$$

We have thus found the two equilibrium points (the Lagrange points L_4 and L_5). These are stable equilibrium points.

The remaining points are found by setting $y = 0$ and $z = 0$, which satisfy equation. Then equation 2.33 becomes,

$$f(x) = \mu\,\frac{(x-1+\mu)}{|x-1+\mu|^3} + (1-\mu)\,\frac{(x+\mu)}{|x+\mu|^3} - x = 0 \tag{2.40}$$

The roots of $f(x) = 0$ yield the other equilibrium points (L_1, L_2, L_3). To find them, one first requires specifying a value for the mass μ and then using a numerical technique to obtain the root for that particular value.

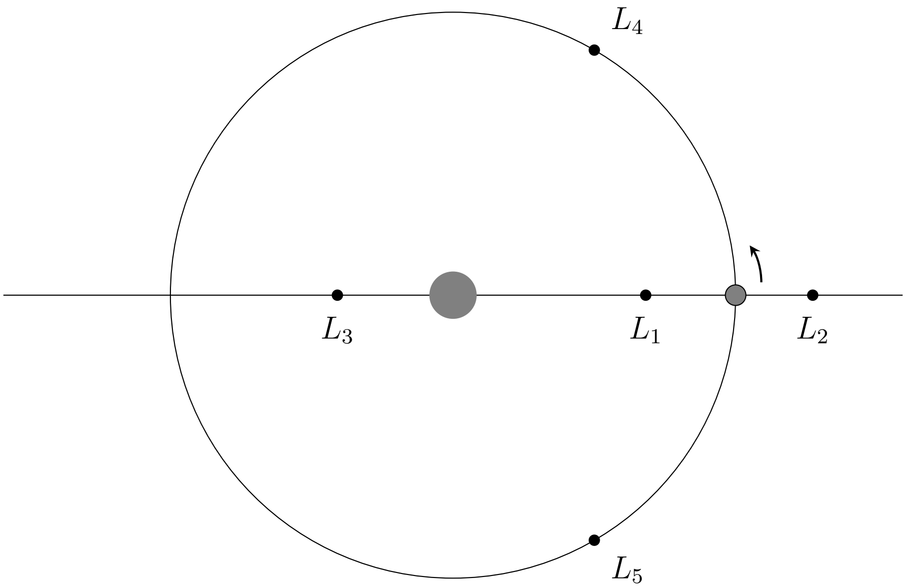

Figure 2.3: Positions of five Lagrange points in the planar CR3BP.

2.5.1 Jacobi Constant

The effective potential U in CR3BP is defined as [32] ,

$$U = \frac{1}{2}(x^2 + y^2) + \frac{1-\mu}{r_1} + \frac{\mu}{r_2}. \tag{2.41}$$

Differentiating U w.r.t 'x' implies,

$$\frac{\partial U}{\partial x} = x - \frac{(1-\mu)(x-x_1)}{r_1^3} - \frac{\mu(x-x_2)}{r_2^3}. \tag{2.42}$$

Differentiating the effective potential w.r.t 'y' implies,

$$\frac{\partial U}{\partial y} = y - \left(\frac{1-\mu}{r_1^3} + \frac{\mu}{r_2^3}\right) y, \tag{2.43}$$

and by differentiating 2.41 w.r.t z we obtain,

$$\frac{\partial U}{\partial z} = -\left(\frac{1-\mu}{r_1^3} + \frac{\mu}{r_2^3}\right) z. \tag{2.44}$$

These are equations of motion for restricted third body in the rotating coordinate system..

Using (2.43) – (2.45) in equations (2.33) we get

$$\left.\begin{aligned} \ddot{x} - 2\dot{y} &= \frac{\partial U}{\partial x}, \\ \ddot{y} + 2\dot{x} &= \frac{\partial U}{\partial y}, \\ \ddot{z} &= \frac{\partial U}{\partial z}. \end{aligned}\right\} \tag{2.45}$$

Multiply equations (2.46) by $\dot{x}$, $\dot{y}$ and $\dot{z}$ respectively and then their sum gives the expression below,

$$\ddot{x}\dot{x} + \ddot{y}\dot{y} + \ddot{z}\dot{z} = \frac{\partial U}{\partial x}\dot{x} + \frac{\partial U}{\partial y}\dot{y} + \frac{\partial U}{\partial z}\dot{z}, \tag{2.46}$$

This forms an exact differential because U depends on x, y and z.

By integration, we further obtain,

$$\dot{x}^2 + \dot{y}^2 + \dot{z}^2 = 2U + C. \tag{2.47}$$

The left hand side of above equation corespnds to the square of velocity of secondary body. So,

$$v^2 = 2U + C. \tag{2.48}$$

This relation is known as the Jacobi integral and is often referred to as the energy in the rotating frame. Since $V^2 \geq 0$ so motion is only allowed where $2U \geq C$, where C is known as Jaccobi Constant.

Here we have the Hill regions for a test particle for multiple values of jacobi constant C. The shaded region represents the forbidden zone of motion and + denotes the Lagrange points of test particle.

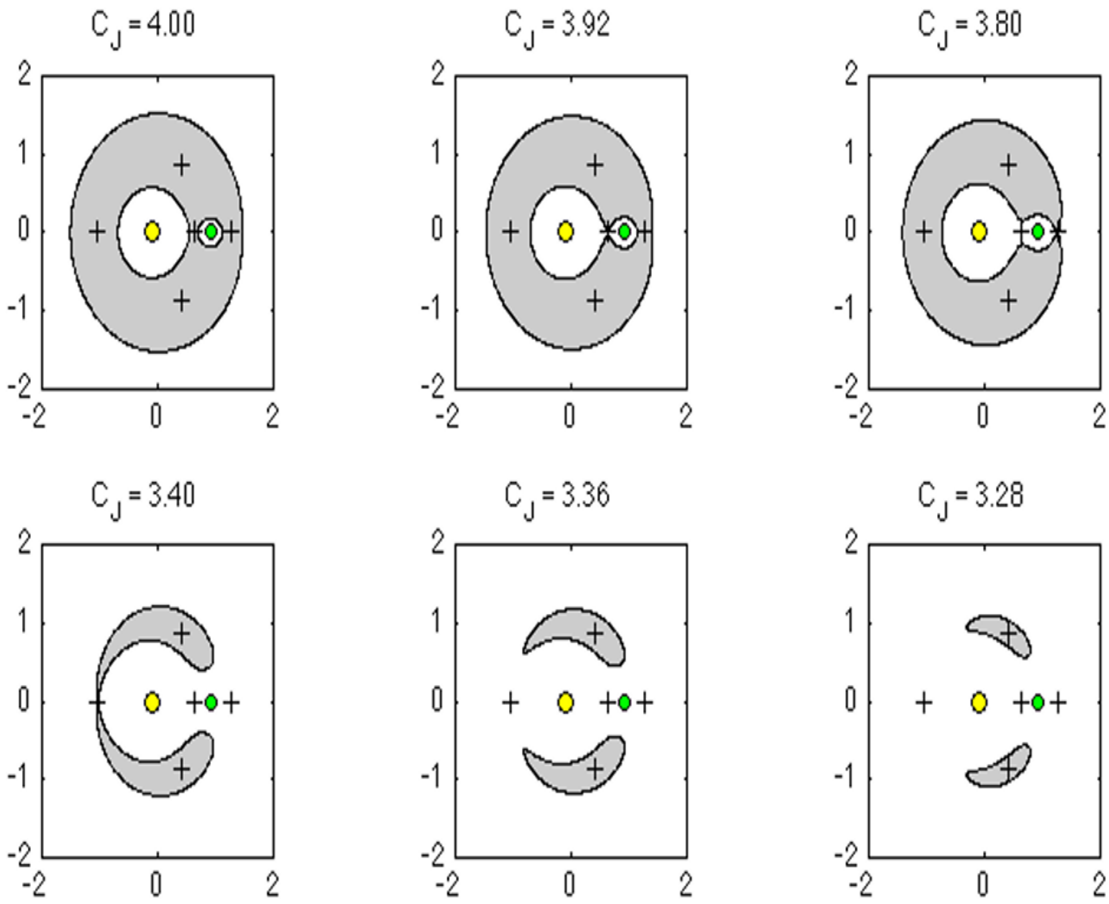

Figure 2.4: Regions of motion (white regions) of test mass in CR3BP for decreasing Jacobi Constant C.

2.6 Central Configuration

In the Newtonian NBP, central configuration refers to a special arrangement of masses in which the net gravitational acceleration acting on each body due to the gravitational attraction of all the other bodies points directly toward the center of mass (CoM) and remains proportional to its distance from the COM.

This condition can be expressed mathematically as,

$$\ddot{\mathbf{r}}_i = -k\,\mathbf{r}_i, \tag{2.49}$$

where k is a scalar proportionality factor that remains identical for all bodies in the system. CC is important because it gives the known exact explicit solutions to the NBP. The main geometrical types of CC for many bodies that have been studied are collinear configurations, regular polygons, trapezoidal shapes, rhombus/kite configurations, spatial configurations, etc [33].

2.6.1 Rhomboidal Central Configuration

It is a specific geometric arrangement of masses where four bodies are located at the vertices of a rhombus while the fifth one is positioned at the point where the diagonals intersects. It provides symmetrical solutions in five-body and six-body gravitational systems such as star-cluster dynamics. In this setup of celestial bodies, the System's gravitational forces are perfectly balanced, allowing the bodies to maintain their symmetric configuration as the system scales or rotates. [34].

Chapter 3

Equilibrium Solutions of Rhomboidal Restricted Six Body Problem

Following the discussion in [26] , this chapter examines the central configuration composed by five primary masses, where $M_1 = M_2 = M_3 = M$ and $M_4 = M_5 = \tilde{M}$. Four primary bodies are placed at the vertices of rhombus with one additional mass situated at the point where diagonals of rhombus intersects. Using the condition of Central Configuration CC, we formulate the mass-ratio function and discuss its interval of continuity and highlight several particular cases. After that, we place a test mass m_0 in the gravitational field of the rhomboidal primary masses and derive the corresponding equations of motion. The chapter concludes by determining the equilibrium points for different parameter values.

3.1 Planar Rhomboidal Central Configuration of Five Primaries

We consider a 2D rotating coordinate system and five primary masses arranged in such a way that the four outer masses M_2, M_3, M_4 and M_5 form the vertices of a rhombus. M_1 is located at the origin, acting as the geometric center of the system. Masses M_2 and M_3 are located symmetrically at the x-axis with position $(a, 0)$ and $(-a, 0)$ respectively given a separation of $2a$. Similarly, M_4 and M_5 lie at y-axis with coordinates $(0, b)$ and $(0, -b)$, and the distance between them is $2b$.

The configuration exhibits reflectional symmetry across both the x- and y-axes and rotational symmetry of 180° about the origin, i.e., D_{2h} symmetry (see Figure 3.1).

The line segments $\overline{M_2M_3}$ and $\overline{M_4M_5}$ serve as the diagonals of the rhombus, which bisect each other perpendicularly at the origin.

We choose three of the primaries of equal masses, i.e., $M_1 = M_2 = M_3 = M$, and the other two primary bodies having the same mass, i.e., $M_4 = M_5 = \tilde{M}$.

All the masses interact gravitationally with each other, and their motion can be completely determined by these interactions.

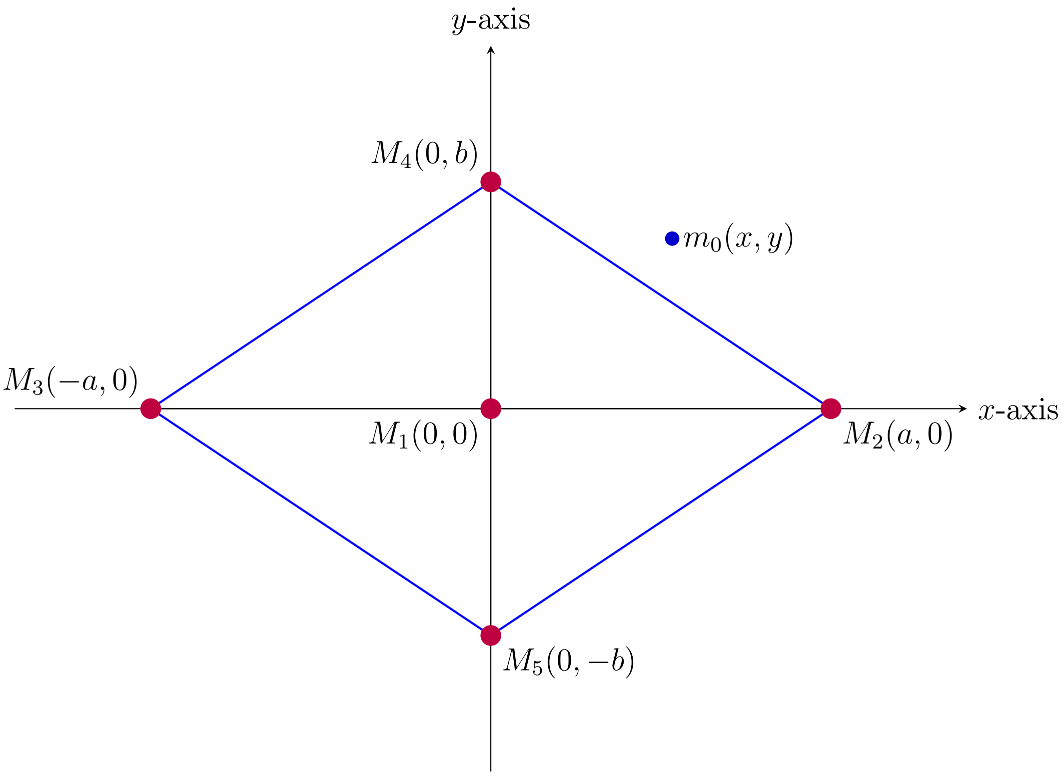

Figure 3.1: Rhomboidal central configuration of five primaries with an infinitesimal mass m_0.

3.2 Existence and Uniqueness of Central Configuration

To model the equations of motion for five primary masses, we consider the gravitational interaction between them. The acceleration of each body is governed by the universal law of gravitation proposed by Newton which can be written as,

$$M_i\ddot{\mathbf{r}}_i = G\sum_{\substack{j=0\\ j\neq i}}^{n} M_i M_j \frac{(\mathbf{r}_j - \mathbf{r}_i)}{|\mathbf{r}_j - \mathbf{r}_i|^3}. \tag{3.1}$$

For convenience, we choose the gravitational constant G equal to one. Here $\ddot{\mathbf{r}}_i$ is the acceleration vector of the i^{th} body and M_i is its mass and $\mathbf{r}_i$ are position vectors of five primary bodies. A CC occurs when the net gravitational force on each body is directed towards the COM of the system and is proportional to its distance from that center.For this geometric arrangement of five massive primaries to be CC, it must satisfies the following fundamental condition of CC,

$$-\omega^2(\mathbf{r}_i - c) = \sum_{\substack{j=1\\ j\neq i}}^{5} M_j \frac{(\mathbf{r}_j - \mathbf{r}_i)}{|\mathbf{r}_j - \mathbf{r}_i|^3}, \tag{3.2}$$

where ω denotes the angular speed of $M_i, i = 1, ..., 5$ and c is the COM of N bodies. To make the calculations easy, we choose $c = 0$ (the COM at the origin).

To simplify computations, the mass ratio is written in terms of a and b, we use $i = 2$ and $i = 4$ in equation 3.2. $i = 2$ implies the CC equation for mass M_2,

$$-\omega^2(a,0) = M_1\frac{(\mathbf{r}_1 - \mathbf{r}_2)}{|\mathbf{r}_1 - \mathbf{r}_2|^3} + M_3\frac{(\mathbf{r}_3 - \mathbf{r}_2)}{|\mathbf{r}_3 - \mathbf{r}_2|^3} + M_4\frac{(\mathbf{r}_4 - \mathbf{r}_2)}{|\mathbf{r}_4 - \mathbf{r}_2|^3} + M_5\frac{(\mathbf{r}_5 - \mathbf{r}_2)}{|\mathbf{r}_5 - \mathbf{r}_2|^3}.$$

Substituting the positions gives,

$$-\omega^2(a,0) = M\frac{(-a,0)}{a^3} + M\frac{(-2a,0)}{8a^3} + \tilde{M}\frac{(-a,b)}{(a^2+b^2)^{3/2}} + \tilde{M}\frac{(-a,-b)}{(a^2+b^2)^{3/2}}. \tag{3.3}$$

$i = 4$ implies the CC equation for mass M_4,

$$-\omega^2(0,b) = M_1 \frac{(\mathbf{r}_1 - \mathbf{r}_4)}{|\mathbf{r}_1 - \mathbf{r}_4|^3} + M_2 \frac{(\mathbf{r}_2 - \mathbf{r}_4)}{|\mathbf{r}_2 - \mathbf{r}_4|^3} + M_3 \frac{(\mathbf{r}_3 - \mathbf{r}_4)}{|\mathbf{r}_3 - \mathbf{r}_4|^3} + M_5 \frac{(\mathbf{r}_5 - \mathbf{r}_4)}{|\mathbf{r}_5 - \mathbf{r}_4|^3}.$$

Substituting the positions gives,

$$-\omega^2(0,b) = M\frac{(0,-b)}{b^3} + M\frac{(a,-b)}{(a^2+b^2)^{3/2}} + M\frac{(-a,-b)}{(a^2+b^2)^{3/2}} + \tilde{M}\frac{(0,-2b)}{8b^3}. \tag{3.4}$$

From equation 3.3, taking the x-component (the only non-zero component in the $(a,0)$ direction) we get

$$\begin{aligned}
-\omega^2 a &= -\frac{Ma}{a^3} - \frac{2Ma}{8a^3} - \frac{\tilde{M}a}{(a^2+b^2)^{3/2}} - \frac{\tilde{M}a}{(a^2+b^2)^{3/2}},\\
-\omega^2 a &= -\frac{Ma}{a^3} - \frac{Ma}{4a^3} - \frac{2\tilde{M}a}{(a^2+b^2)^{3/2}},\\
-\omega^2 a &= -\frac{5Ma}{4a^3} - \frac{2\tilde{M}a}{(a^2+b^2)^{3/2}},
\end{aligned}$$

which simplifies to,

$$\omega^2 = \frac{5M}{4a^3} + \frac{2\tilde{M}}{(a^2+b^2)^{3/2}}. \tag{3.5}$$

From equation 3.4, taking the y-component (the only non-zero component in the $(0,b)$ direction) we get,

$$-\omega^2 b = -\frac{Mb}{b^3} - \frac{2Mb}{(a^2+b^2)^{3/2}} - \frac{\tilde{M}b}{4b^3},$$

which simplifies to,

$$\omega^2 = M\left(\frac{1}{b^3} + \frac{2}{(a^2+b^2)^{3/2}}\right) + \frac{\tilde{M}}{4b^3}. \tag{3.6}$$

Due to the symmetry of the rhomboidal configuration, the equations for masses M_3 and M_5 are identical to equations 3.5 and 3.6 respectively. The CC equation for M_1 is identically zero. For simplicity, we normalize the angular velocity (i.e., $\omega = 1$) and simultaneously solving equations 3.5 and 3.6 for M and $\tilde{M}$ we obtain the following,

$$\left.\begin{aligned} M(a,b) &= \frac{N_M(a,b)}{D_M(a,b)}, \\ \tilde{M}(a,b) &= \frac{N_{\tilde{M}}(a,b)}{D_M(a,b)}, \end{aligned}\right\} \tag{3.7}$$

where,

$$N_M(a,b) = 4a^3(a^2+b^2)^{3/2}\left((a^2+b^2)^{3/2} - 8b^3\right), \tag{3.8}$$

and,

$$\begin{aligned} N_{\tilde{M}}(a,b) = 4(a^2+b^2)^{3/2}\big(&-4a^7 - 8a^5b^2 + 5a^4b^3 - 4a^3b^4 + 10a^2b^5 \\ &- 8a^3b^3\sqrt{a^2+b^2} + 5b^7\big), \end{aligned} \tag{3.9}$$

$$\begin{aligned} D_M(a,b) = &-32a^7 - 64a^5b^2 - 32a^3b^4 + \left(5a^6 + 15a^4b^2 - 64a^3b^3\right. \\ &\left.+ 15a^2b^4 + 5b^6\right)\sqrt{a^2+b^2}. \end{aligned} \tag{3.10}$$

Let us define $\tau = \dfrac{\tilde{M}}{M}$; then equations 3.7 through 3.10 give,

$$\tau(a,b) = \frac{8\left(\dfrac{b^3}{a^3}\right) + \left(4 - 5\dfrac{b^3}{a^3}\right)\left(1 + \dfrac{b^2}{a^2}\right)^{3/2}}{8\left(\dfrac{b^3}{a^3}\right) - \left(1 + \dfrac{b^2}{a^2}\right)^{3/2}}. \tag{3.11}$$

Now defining $\mu = \dfrac{b}{a}$ in equation 3.11, we get the equation in the form

$$\tau(\mu) = \frac{8\mu^3 + (4 - 5\mu^3)(1+\mu^2)^{3/2}}{8\mu^3 - (1+\mu^2)^{3/2}}. \tag{3.12}$$

3.3 Interval of Continuity for Mass Ratio Function

It can be verified that the function $\tau(\mu)$ is continuous, strictly decreasing and positive function over the interval $\left(\dfrac{1}{\sqrt{3}},\ 1.1394282249562009\right)$.

By taking some random values from the given interval like $\mu = 0.6,\ 0.8,\ 1,\ 1.3$ etc., we see that the denominator

$$D = 8\mu^3 - \left(1+\mu^2\right)^{3/2} < 0,$$

and also the numerator

$$N = 8\mu^3 + \left(4 - 5\mu^3\right)\left(1+\mu^2\right)^{3/2} < 0.$$

Hence $\tau = \dfrac{N}{D} > 0$, so $\tau(\mu)$ is always positive.

$\tau(\mu)$ is strictly decreasing if $\tau'(\mu) < 0$. After differentiation and simplification, we get,

$$\tau'(\mu) = \frac{-12\,\mu\sqrt{1+\mu^2}\left[4\mu^2\left(1+\mu^2\right) + \left(4-7\mu^2\right)\left(1+\mu^2\right)^{3/2} + 2\mu^2\right]}{\left[8\mu^3 - \left(1+\mu^2\right)^{3/2}\right]^2}.$$

Here the denominator is always positive being the square of a value i.e. $D > 0$. The expression in the bracket is positive because it μ is squared, but the term $-12\,\mu\sqrt{1+\mu^2}$ is negative for $\mu > 0$ so $N < 0$. Finally, we have $\tau'(\mu) < 0$ everywhere it is defined in the given interval, that is, strictly decreasing.

3.3.1 Particular Cases

We consider two extreme cases where the rhomboidal central configuration (CC) of five primaries breaks down.

(i) For $\mu = 1.1394282249562009$, equation 3.12 returns $\tau = 0$, which implies $\tilde{M} = 0$. Therefore three equal masses $M = M_1 = M_2 = M_3$ remain.

(ii) For $\mu = \dfrac{1}{\sqrt{3}}$ we have $\tau = \infty$. This means that $M = 0$ so in this case, only two primary masses are left on the y-axis.

From the preceding discussion, we note that the value of $\tau(\mu)$, which is the mass ratio will always remain positive thrughout this interval as,

$$\lim_{\mu\to\frac{1}{\sqrt{3}}} \tau(\mu) = \infty \qquad \text{and} \qquad \tau(1.1394282249562009) = 0.$$

So $\tau(\mu) \in [0, \infty)$.

Now we find the value of $\tau(\mu)$ for some particular values of μ.

Case 1: For $\mu = 1$, equation 3.12 returns $\tau = 1$. This yields $M = \tilde{M} = 1$ and $a = b = 1$, corresponding to a perfect square geometry.

Case 2: For $\mu = 1.04232$, equation 3.12 gives $\tau = 0.67$. We then obtain $\tilde{M} = 0.67\, M$ and $b = 1.04232\, a$.

Case 3: For $\mu = 1.00367$ we get $\tau = 0.97$ from equation 3.12. This leads to $\tilde{M} = 0.97\, M$ and $b = 1.00367\, a$.

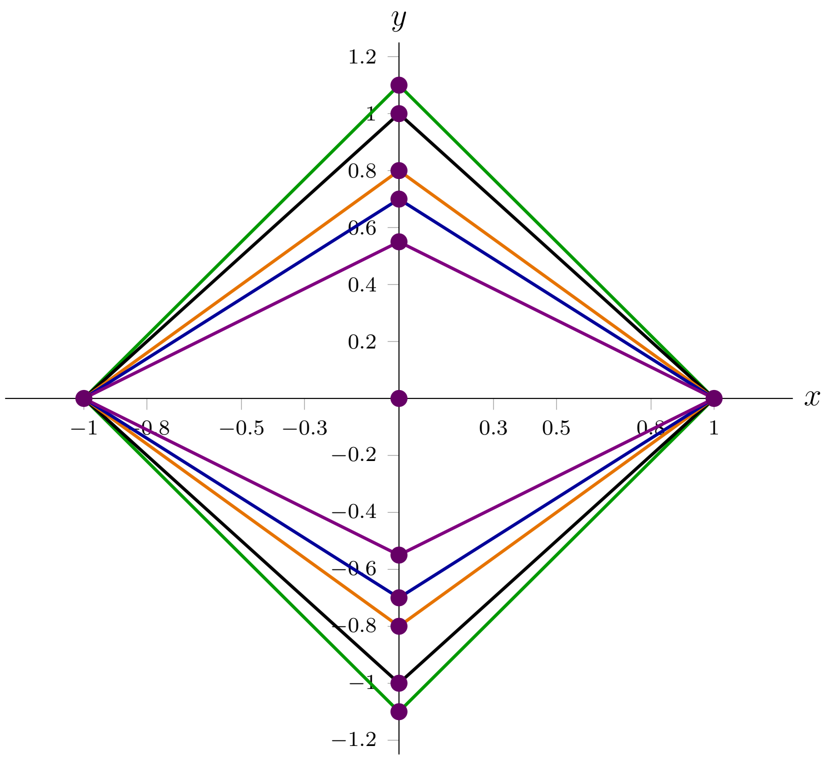

Figure 3.2: Some possible shapes of rhombus for different values of μ.

3.4 Equilibrium Points of Secondary Mass m_0

In this section we analyze the dynamics of an infinitesimal mass m_0 with the position vector $\mathbf{r}_0$ under the gravitational attraction of M_i with positions $\mathbf{r}_i$ where $i = 1, 2, \cdots 5$.

The secondary body of mass m_0 is considered negligible as compared to the primary bodies.

The equations of motion of m_0 in rotating coordinate system are as follows,

$$\left.\begin{aligned} \ddot{x} - 2\dot{y} &= \frac{\partial U}{\partial x}, \\ \ddot{y} + 2\dot{x} &= \frac{\partial U}{\partial y}. \end{aligned}\right\} \tag{3.13}$$

where U is the effective potential defined as,

$$\begin{aligned} U(x,y) = \tfrac{1}{2}\left(x^2+y^2\right) + M\left(\frac{1}{|\boldsymbol{r}_0-\boldsymbol{r}_1|} + \frac{1}{|\boldsymbol{r}_0-\boldsymbol{r}_2|} + \frac{1}{|\boldsymbol{r}_0-\boldsymbol{r}_3|}\right) \\ + \tilde{M}\left(\frac{1}{|\boldsymbol{r}_0-\boldsymbol{r}_4|} + \frac{1}{|\boldsymbol{r}_0-\boldsymbol{r}_5|}\right). \end{aligned} \tag{3.14}$$

The mutual distances of m_0 to the primaries are,

$$\left.\begin{aligned} |\boldsymbol{r}_0-\boldsymbol{r}_1| &= \sqrt{x^2+y^2} \\ |\boldsymbol{r}_0-\boldsymbol{r}_2| &= \sqrt{(x-a)^2+y^2} \\ |\boldsymbol{r}_0-\boldsymbol{r}_3| &= \sqrt{(x+a)^2+y^2} \\ |\boldsymbol{r}_0-\boldsymbol{r}_4| &= \sqrt{x^2+(y-b)^2} \\ |\boldsymbol{r}_0-\boldsymbol{r}_5| &= \sqrt{x^2+(y+b)^2} \end{aligned}\right\} \tag{3.15}$$

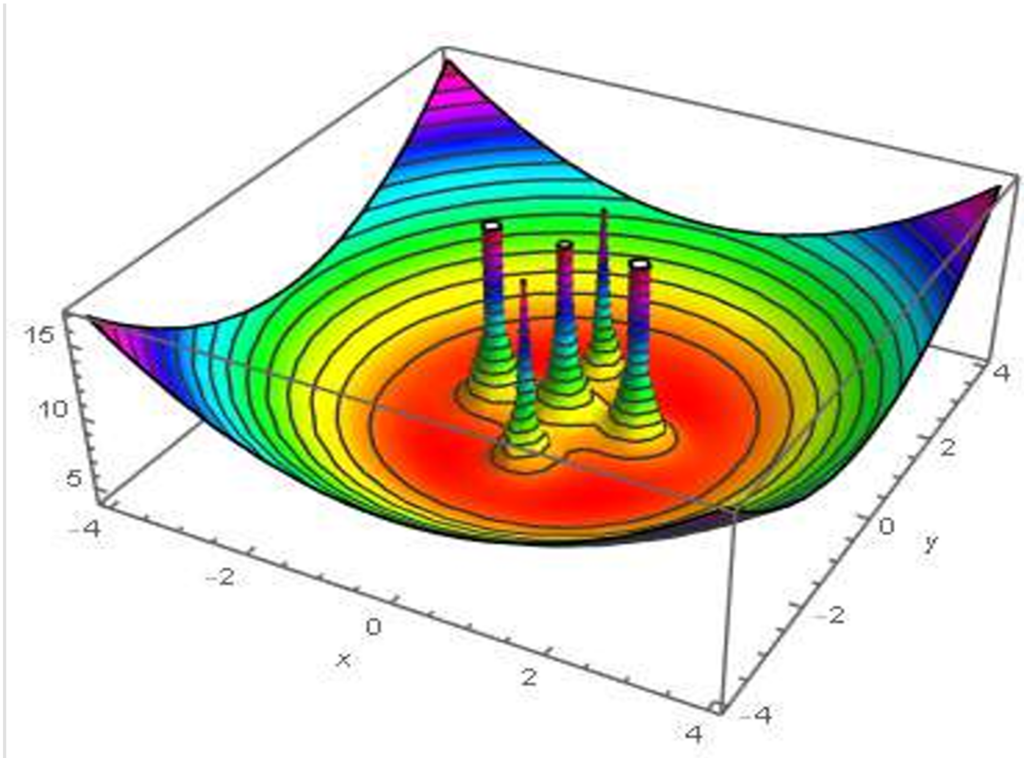

(a)

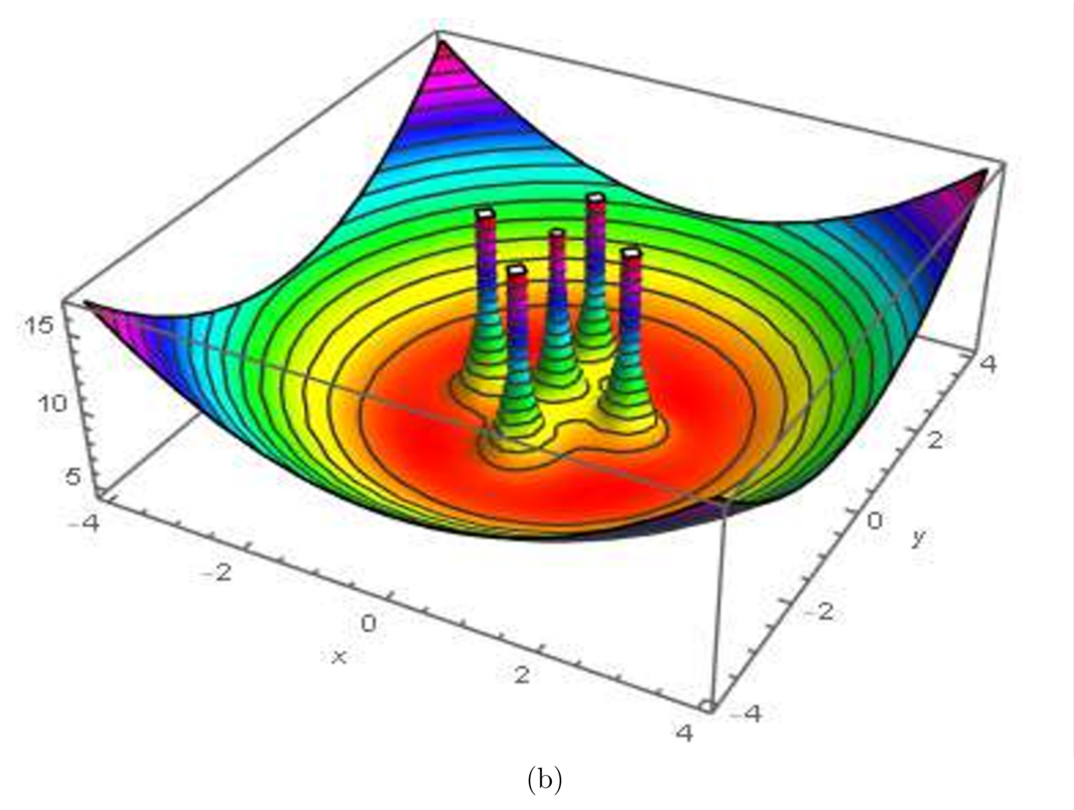

(b)

Figure 3.3: Effective potential: (a) $a = M = 1$, $b = 1.04232$, $\tilde{M} = 0.67$; (b) $a = M = 1$, $b = 1.00367$, $\tilde{M} = 0.97$.

For the RR6BP, equilibrium solutions satisfy $U_x(x,y) = 0$ and $U_y(x,y) = 0$. This follows by setting $\dot{x} = \dot{y} = \ddot{x} = \ddot{y} = 0$ in equation 3.13,

$$\begin{aligned} U_x = x - M\left(\frac{x}{(x^2+y^2)^{3/2}} + \frac{x-a}{\left((x-a)^2+y^2\right)^{3/2}} + \frac{x+a}{\left((x+a)^2+y^2\right)^{3/2}}\right) \\ - \tilde{M}\left(\frac{x}{\left((y-b)^2+x^2\right)^{3/2}} + \frac{x}{\left(x^2+(y+b)^2\right)^{3/2}}\right) = 0, \end{aligned} \tag{3.16}$$

$$\begin{aligned} U_y = y - M\left(\frac{y}{(x^2+y^2)^{3/2}} + \frac{y}{\left((x-a)^2+y^2\right)^{3/2}} + \frac{y}{\left((x+a)^2+y^2\right)^{3/2}}\right) \\ - \tilde{M}\left(\frac{y-b}{\left(x^2+(y-b)^2\right)^{3/2}} + \frac{y+b}{\left(x^2+(y+b)^2\right)^{3/2}}\right) = 0. \end{aligned} \tag{3.17}$$

For the collinear equilibrium points on the x-axis, use $y = 0$ in 3.16 and 3.17; then 3.17 is identically satisfied and 3.16 gives,

$$x - M\left(\frac{1}{x^2} + \frac{1}{(x-a)^2} + \frac{1}{(x+a)^2}\right) - \tilde{M}\left(\frac{2x}{(x^2+b^2)^{3/2}}\right) = 0. \tag{3.18}$$

Similarly, for getting points on y-axis we put $x = 0$ in equations 3.16 and 3.17. We see that 3.16 is satisfied and 3.17 returns,

$$y - M\left(\frac{1}{y^2} + \frac{2y}{(a^2+y^2)^{3/2}}\right) - \tilde{M}\left(\frac{1}{(y-b)^2} + \frac{1}{(y+b)^2}\right) = 0. \tag{3.19}$$

The off-axis equilibrium points can be obtained by solving 3.16 and 3.17 simultaneously. But this is very challenging to solve these equations analytically because the $(x^2+y^2)^{3/2}$ terms make them high degree, and the Abel-Ruffini theorem [35] says that polynomials having degree 5 or higher generally have no closed-form solution with radicals.

We can solve the above equations using iterative methods such as the Newton-Raphson method or other standard methods for nonlinear systems. But these methods involve complex calculations and are sensitive to initial values. To avoid these complications and to achieve accurate results we directly used the software

Mathematica which has efficient built-in numerical solvers that can directly handle nonlinear coupled equations. The results for all three cases are given in Table 3.1.

Table 3.1: Equilibrium points for three cases of shape and mass parameters.

Equilibrium points	**Case 1**	**Case 2**	**Case 3**
L_1	$(0,\ 0.51991)$	$(0,\ 0.59052)$	$(0,\ 0.52541)$
L_2	$(0,\ -0.51991)$	$(0,\ -0.59052)$	$(0,\ -0.52541)$
L_3	$(0,\ 1.92684)$	$(0,\ 1.83761)$	$(0,\ 1.91963)$
L_4	$(0,\ -1.92684)$	$(0,\ -1.83761)$	$(0,\ -1.91963)$
L_5	$(0.51991,\ 0)$	$(0.51137,\ 0)$	$(0.51907,\ 0)$
L_6	$(-0.51991,\ 0)$	$(-0.51137,\ 0)$	$(-0.51907,\ 0)$
L_7	$(1.92684,\ 0)$	$(1.89551,\ 0)$	$(1.92391,\ 0)$
L_8	$(-1.92684,\ 0)$	$(-1.89551,\ 0)$	$(-1.92391,\ 0)$
L_9	$(1.21443,\ 1.21443)$	$(1.04556,\ 1.23821)$	$(1.20045,\ 1.21691)$
L_{10}	$(-1.21443,\ 1.21443)$	$(-1.04556,\ 1.23821)$	$(-1.04556,\ 1.23821)$
L_{11}	$(1.21443,\ -1.21443)$	$(1.04556,\ -1.23821)$	$(1.20045,\ -1.21691)$
L_{12}	$(-1.21443,\ -1.21443)$	$(-1.04556,\ -1.23821)$	$(-1.20045,\ -1.21691)$

Table 3.1 lists the 12 planar equilibrium points for Cases 1, 2, and 3. The points L_1 to L_8 lie on the coordinate axes, while L_9 to L_{12} are off-axes points located symmetrically in the four quadrants. Comparison of the three cases shows that changing the rhombus geometry or central mass shifts the locations of equilibrium points.

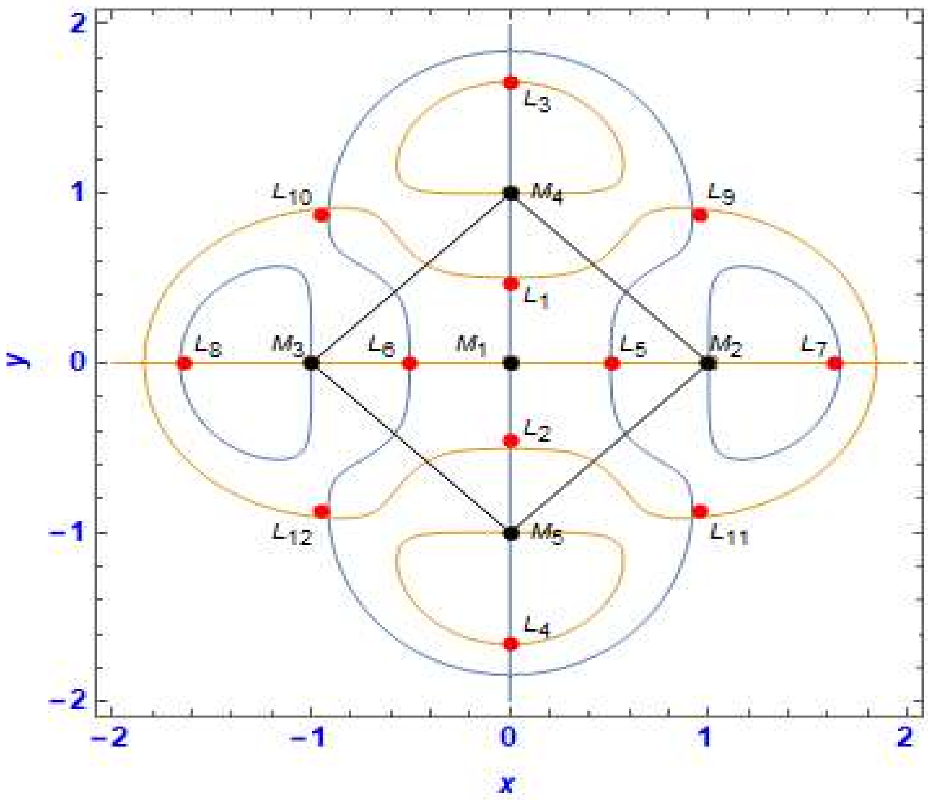
L3
M4
L10
L9
L1
L8
M3
L6
M1
L5
M2
L7
L2
L12
M5
L11
L4
y
x
2
1
0
−1
−2
2
1
0
−1
−2

(a)

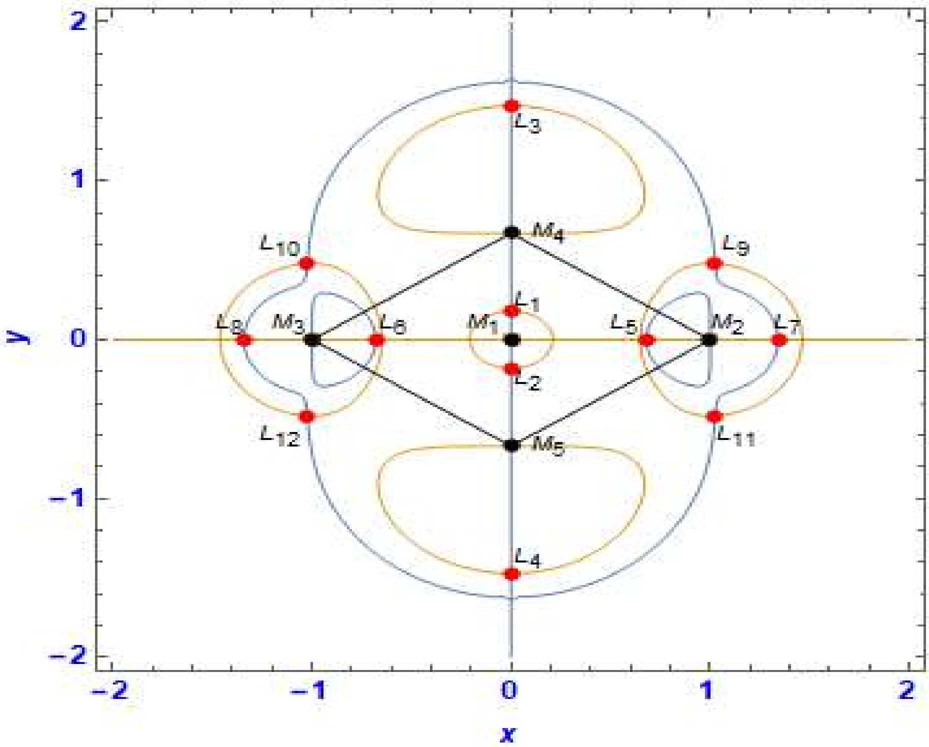
L3
M4
L10
L9
L1
L8
M3
L6
M1
L5
M2
L7
L2
L12
M5
L11
L4
y
x
2
1
0
−1
−2
2
1
0
−1
−2

(b)

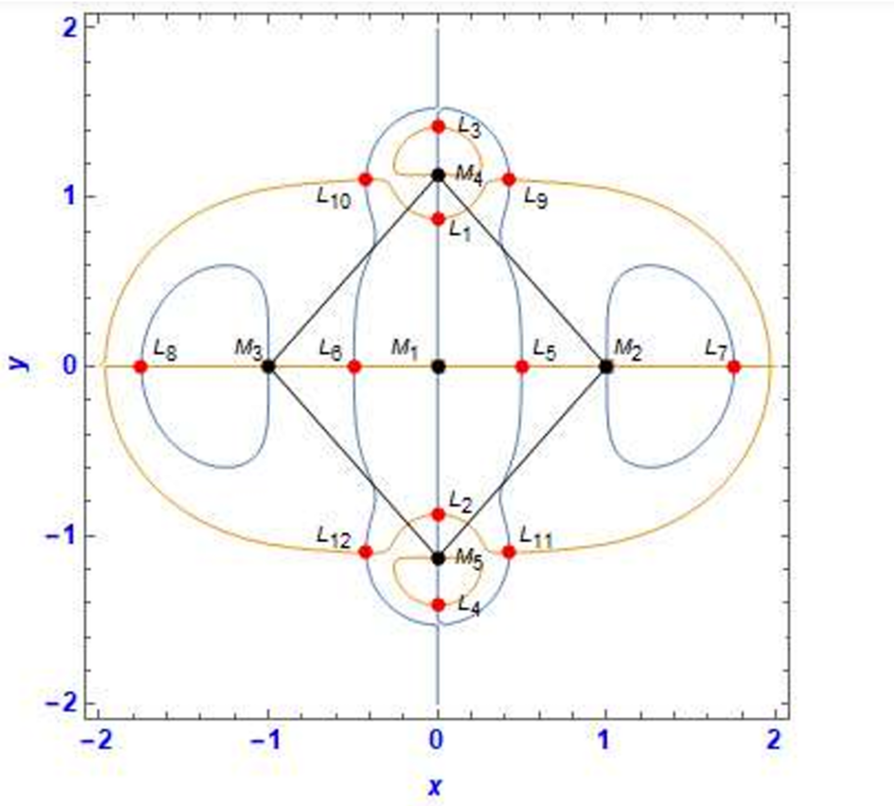

(c)

Figure 3.4: Equilibrium points distribution for three different rhombus geometries.

The above figures illustrate the locations of equilibrium points (red dots) for mass m_0. The black rhombus connects the four outer primary masses. The blue and orange curves are ZVCs for the selected values of Jacobi constant C. The positions of the equilibrium points depend on the rhombus aspect ratio b/a. Since the effective potential depends on both mass and distance parameters, therefore the positions of equilibrium points shift relative to the primary masses as b takes different values.

Chapter 4

Motion of Two Secondary Bodies in the Rhomboidal Central Configuration of Five Primaries

In this extended study, we derive the equations of motion for the secondary bodies having masses m_1 and m_2, taking into account their mutual gravitational interaction as well as the gravitational influence of the rhomboidal central configuration of five primary masses.

This formulation yields a coupled system of nonlinear algebraic equations, which is solved numerically. The main objectives of this study are to find the equilibrium solutions, investigate their stability, and identify the corresponding possible regions of motion.

4.1 Equations of Motion of Two Secondary Bodies

Consider two infinitesimal bodies, designated as m_1 having the position (x_1, y_1) and m_2 with the position vector (x_2, y_2). These bodies have negligible mass as compared to primary bodies. They are attracted by the rhomboidal primaries, but do not gravitationally affect them (see Figure 4.1).

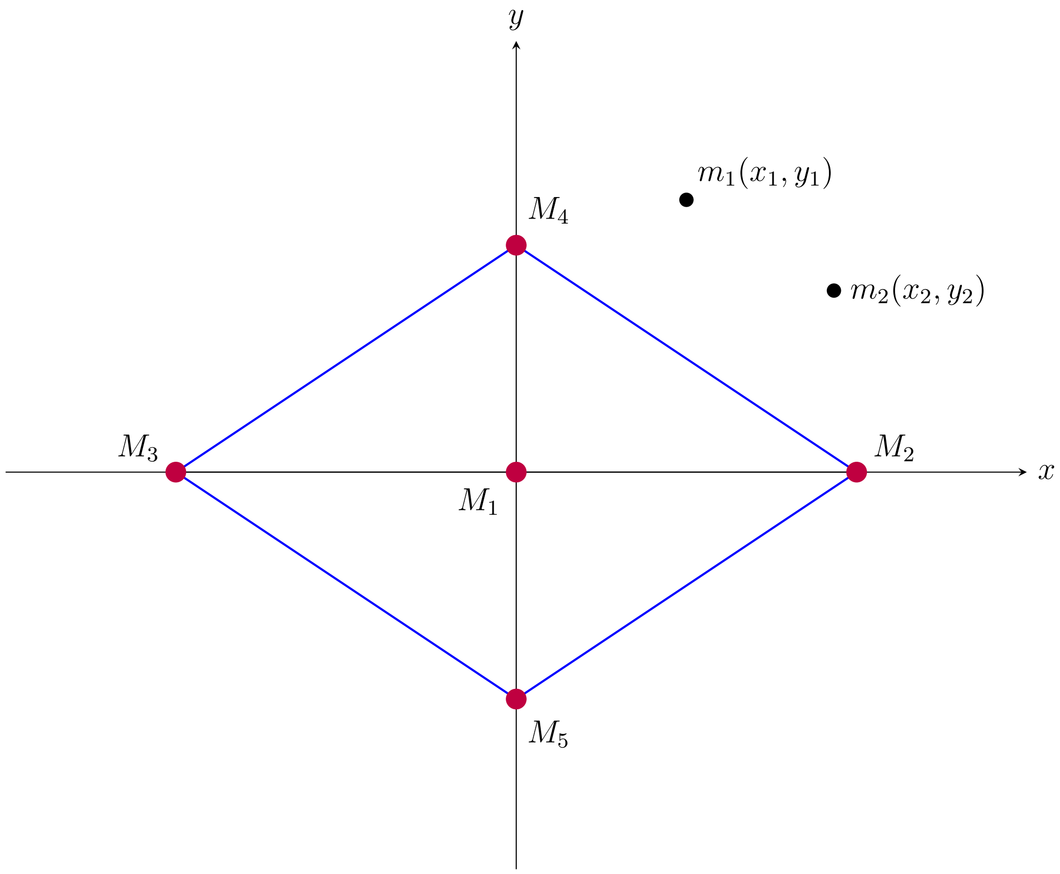

Figure 4.1: Restricted rhomboidal 5 + 2-body problem.

In the rotating coordinate system, we model the equation of motion for each secondary body m_α, where $\alpha = 1, 2$. The governing equations are

$$\ddot{x}_\alpha - 2\dot{y}_\alpha = \frac{\partial T}{\partial x_\alpha}, \tag{4.1}$$

$$\ddot{y}_\alpha + 2\dot{x}_\alpha = \frac{\partial T}{\partial y_\alpha}, \tag{4.2}$$

where T is the effective potential. It combines the true potential energy with rotational (centrifugal) effects and allows the simplification of complex multi-dimensional orbital problems. Here, this effective potential is written as,

$$T = \sum_{\alpha=1}^{2} m_\alpha \left[\frac{1}{2} \left(x_\alpha^2 + y_\alpha^2 \right) + \sum_{i=1}^{5} \frac{M_i}{|\mathbf{p}_\alpha - \mathbf{r_i}|} \right] + \sum_{1 \leq \alpha < \beta \leq 2} \frac{m_\alpha m_\beta}{|\mathbf{p}_\alpha - \mathbf{p}_\beta|}. \tag{4.3}$$

the term $\displaystyle\sum_{1\leq\alpha<\beta\leq 2} \frac{m_\alpha m_\beta}{|\mathbf{p}_\alpha - \mathbf{p}_\beta|}$ represents the mutual gravitational interaction of the secondaries bodies. Here $\mathbf{p}_\alpha$ and $\mathbf{p}_\beta$ are the position vectors of the test masses and $\boldsymbol{r}_i$ are the position vectors of primary masses M_i (i=1,2,...5).

Expanding equation 4.3 gives

$$
\begin{aligned}
T = m_1 \Bigg[\frac{1}{2}\left(x_1^2 + y_1^2\right) &+ M\left(\frac{1}{|\mathbf{p_1} - \mathbf{r_1}|} + \frac{1}{|\mathbf{p_1} - \mathbf{r_2}|} + \frac{1}{|\mathbf{p_1} - \mathbf{r_3}|}\right) \\
&+ \tilde{M}\left(\frac{1}{|\mathbf{p_1} - \mathbf{r_4}|} + \frac{1}{|\mathbf{p_1} - \mathbf{r_5}|}\right)\Bigg] \\
+ m_2 \Bigg[\frac{1}{2}\left(x_2^2 + y_2^2\right) &+ M\left(\frac{1}{|\mathbf{p_2} - \mathbf{r_1}|} + \frac{1}{|\mathbf{p_2} - \mathbf{r_2}|} + \frac{1}{|\mathbf{p_2} - \mathbf{r_3}|}\right) \\
&+ \tilde{M}\left(\frac{1}{|\mathbf{p_2} - \mathbf{r_4}|} + \frac{1}{|\mathbf{p_2} - \mathbf{r_5}|}\right)\Bigg] \\
+ \frac{m_1 m_2}{|\mathbf{p_1} - \mathbf{p_2}|}&,
\end{aligned}
\tag{4.4}
$$

where,

$$
\begin{aligned}
|\mathbf{p_1} - \mathbf{r_1}| &= \sqrt{x_1^2 + y_1^2}, & |\mathbf{p_2} - \mathbf{r_1}| &= \sqrt{x_2^2 + y_2^2}, \\
|\mathbf{p_1} - \mathbf{r_2}| &= \sqrt{(x_1 - a)^2 + y_1^2}, & |\mathbf{p_2} - \mathbf{r_2}| &= \sqrt{(x_2 - a)^2 + y_2^2}, \\
|\mathbf{p_1} - \mathbf{r_3}| &= \sqrt{(x_1 + a)^2 + y_1^2}, & |\mathbf{p_2} - \mathbf{r_3}| &= \sqrt{(x_2 + a)^2 + y_2^2}, \\
|\mathbf{p_1} - \mathbf{r_4}| &= \sqrt{x_1^2 + (y_1 - b)^2}, & |\mathbf{p_2} - \mathbf{r_4}| &= \sqrt{x_2^2 + (y_2 - b)^2}, \\
|\mathbf{p_1} - \mathbf{r_5}| &= \sqrt{x_1^2 + (y_1 + b)^2}, & |\mathbf{p_2} - \mathbf{r_5}| &= \sqrt{x_2^2 + (y_2 + b)^2},
\end{aligned}
$$

with $M = M_1 = M_2 = M_3$ and $\tilde{M} = M_4 = M_5$, and

$$
|\mathbf{p}_1 - \mathbf{p}_2| = \sqrt{(x_1 - x_2)^2 + (y_1 - y_2)^2}.
$$

The equilibrium solutions of the system are obtained by imposing the condition that all the velocities and accelerations vanish in the equations of motion. So,

$$
\dot{x}_\alpha = \dot{y}_\alpha = \ddot{x}_\alpha = \ddot{y}_\alpha = 0, \qquad \text{for } \alpha = 1, 2.
$$

in equations equations 4.1 and 4.2 we get,

$$\frac{\partial T}{\partial x_\alpha} = 0, \tag{4.5}$$

$$\frac{\partial T}{\partial y_\alpha} = 0. \tag{4.6}$$

The partial derivatives of T give the equations that define the locations of the equilibrium solutions:

$$\begin{aligned} x_1 - M\left(\frac{x_1}{|\boldsymbol{p}_1 - \boldsymbol{r}_1|^3} + \frac{x_1 - a}{|\boldsymbol{p}_1 - \boldsymbol{r}_2|^3} + \frac{x_1 + a}{|\boldsymbol{p}_1 - \boldsymbol{r}_3|^3}\right) \\ - \tilde{M}\left(\frac{x_1}{|\boldsymbol{p}_1 - \boldsymbol{r}_4|^3} + \frac{x_1}{|\boldsymbol{p}_1 - \boldsymbol{r}_5|^3}\right) - \frac{m_2(x_1 - x_2)}{|\boldsymbol{p}_1 - \boldsymbol{p}_2|^3} = 0, \end{aligned} \tag{4.7}$$

$$\begin{aligned} x_2 - M\left(\frac{x_2}{|\boldsymbol{p}_2 - \boldsymbol{r}_1|^3} + \frac{x_2 - a}{|\boldsymbol{p}_2 - \boldsymbol{r}_2|^3} + \frac{x_2 + a}{|\boldsymbol{p}_2 - \boldsymbol{r}_3|^3}\right) \\ - \tilde{M}\left(\frac{x_2}{|\boldsymbol{p}_2 - \boldsymbol{r}_4|^3} + \frac{x_2}{|\boldsymbol{p}_2 - \boldsymbol{r}_5|^3}\right) + \frac{m_1(x_1 - x_2)}{|\boldsymbol{p}_1 - \boldsymbol{p}_2|^3} = 0, \end{aligned} \tag{4.8}$$

$$\begin{aligned} y_1 - M\left(\frac{y_1}{|\boldsymbol{p}_1 - \boldsymbol{r}_1|^3} + \frac{y_1}{|\boldsymbol{p}_1 - \boldsymbol{r}_2|^3} + \frac{y_1}{|\boldsymbol{p}_1 - \boldsymbol{r}_3|^3}\right) \\ - \tilde{M}\left(\frac{y_1 - b}{|\boldsymbol{p}_1 - \boldsymbol{r}_4|^3} + \frac{y_1 + b}{|\boldsymbol{p}_1 - \boldsymbol{r}_5|^3}\right) - \frac{m_2(y_1 - y_2)}{|\boldsymbol{p}_1 - \boldsymbol{p}_2|^3} = 0, \end{aligned} \tag{4.9}$$

$$\begin{aligned} y_2 - M\left(\frac{y_2}{|\boldsymbol{p}_2 - \boldsymbol{r}_1|^3} + \frac{y_2}{|\boldsymbol{p}_2 - \boldsymbol{r}_2|^3} + \frac{y_2}{|\boldsymbol{p}_2 - \boldsymbol{r}_3|^3}\right) \\ - \tilde{M}\left(\frac{y_2 - b}{|\boldsymbol{p}_2 - \boldsymbol{r}_4|^3} + \frac{y_2 + b}{|\boldsymbol{p}_2 - \boldsymbol{r}_5|^3}\right) + \frac{m_1(y_1 - y_2)}{|\boldsymbol{p}_1 - \boldsymbol{p}_2|^3} = 0. \end{aligned} \tag{4.10}$$

Equations 4.7–4.10 form a coupled nonlinear algebraic system that is not possible to solve analytically.

Real solutions of these equations correspond to the equilibrium points of the planar restricted rhomboidal $5+2$ body problems.

4.2 Evaluation of Equilibrium Points by following Perturbation Approach

Whipple [9] presented expressions for locating the equilibrium points of the restricted $2+2$ body problem by using the classical Lagrange points of the CR3BP as initial approximations. Following the same approach, we adapt those formulae for the restricted $5+2$ body problem.

For this purpose, the effective potential of the Rhomboidal Restricted Six-Body Problem (RR6BP) together with the corresponding equilibrium points L_i ($i = 1, 2, \ldots, 12$) listed in Table 3.1 serve as the initial approximations for determining the equilibrium configurations for the two secondary bodies of masses m_1 and m_2.

It is convenient to classify the equilibrium solutions into three categories. The first category consists of equilibrium points located near the four equilibrium points on the y-axis, namely L_1, L_2, L_3, and L_4. The second category consists of equilibrium points located near the four collinear equilibrium points on the x-axis, namely L_5, L_6, L_7, and L_8. Finally, the third category consists of the off-axis equilibrium points located near L_9, L_{10}, L_{11}, and L_{12}.

By inspection, equations (4.7) and (4.8) are identically satisfied when $x_1 = x_2 = 0$. It therefore remains to determine y_1 and y_2 from equations (4.9) and (4.10), which reduce to

$$y_1 - M\left[\frac{1}{y_1^2} + \frac{2y_1}{(y_1^2+a^2)^{3/2}}\right] - \tilde{M}\left[\frac{1}{(y_1-b)^2} + \frac{1}{(y_1+b)^2}\right] - \frac{m_2}{(y_1-y_2)^2} = 0, \quad (4.11)$$

$$y_2 - M\left[\frac{1}{y_2^2} + \frac{2y_2}{(y_2^2+a^2)^{3/2}}\right] - \tilde{M}\left[\frac{1}{(y_2-b)^2} + \frac{1}{(y_2+b)^2}\right] + \frac{m_1}{(y_1-y_2)^2} = 0. \quad (4.12)$$

The solution of these equations are given by using Taylor's expansion about L_i upto first-order approximation. Let $y(L_i)$ be the y-coordinate of the equilibrium point. We write,

$$y_1 = y(L_i) + \epsilon_1$$
$$y_2 = y(L_i) + \epsilon_2$$

where ϵ_1 and ϵ_2 are small perturbations due to mutual interaction between the two test particles. Define the function for a single particle (without mutual interaction),

$$f(y) = y - M\left(\frac{1}{y^2} + \frac{2y}{(a^2+y^2)^{3/2}}\right) - \tilde{M}\left(\frac{1}{(y-b)^2} + \frac{1}{(y+b)^2}\right) = 0.$$

At equilibrium for the uncoupled case, we have,

$$f(y(L_i)) = 0.$$

Making the substitution of $y_1 = y(L_i) + \epsilon_1$ in (4.11) we obtain,

$$f(y(L_i) + \epsilon_1) - \frac{m_2}{(\epsilon_1 - \epsilon_2)^2} = 0.$$

Now expand $f(y(L_i) + \epsilon_1)$ in Taylor series about $y(L_i)$,

$$f(y(L_i) + \epsilon_1) = f(y(L_i)) + f'(y(L_i))\epsilon_1 + \frac{f''(y(L_i))}{2!}\epsilon_1^2 + \cdots$$

Since ϵ_1 is small, we keep only the linear term (first-order approximation). So,

$$f(y(L_i) + \epsilon_1) \approx f(y(L_i)) + f'(y(L_i))\epsilon_1$$

But $f(y(L_i)) = 0$. Hence,

$$f(y(L_i) + \epsilon_1) \approx f'(y(L_i))\epsilon_1.$$

Now, note that $f'(y(L_i)) = U_{yy}(L_i)$ because $U(x, y)$ is the effective potential and U_{yy} is its second partial derivative with respect to y, which equals $f'(y)$ for the single-particle case.

Therefore,

$$U_{yy}(L_i)\epsilon_1 - \frac{m_2}{(\epsilon_1 - \epsilon_2)^2} = 0.$$

Which implies,

$$\boxed{U_{yy}(L_i)\epsilon_1 = \frac{m_2}{(\epsilon_1 - \epsilon_2)^2}}$$

The left-hand side $U_{yy}(L_i)\epsilon_1$ represents the restoring force from the primaries when $m_1$is displaced from the equilibrium point by ϵ_1 and the right-hand side $\frac{m_2}{(\epsilon_1-\epsilon_2)^2}$ represents the gravitational attraction from m_2.

Now, substitute $y_2 = y(L_i) + \epsilon_2$ in equation (4.12), which returns:

$$f(y(L_i) + \epsilon_2) + \frac{m_1}{(\epsilon_1 - \epsilon_2)^2} = 0$$

Now expand $f(y(L_i) + \epsilon_2)$ in Taylor series,

$$f(y(L_i) + \epsilon_2) \approx f(y(L_i)) + f'(y(L_i))\epsilon_2.$$

Using $f(y(L_i)) = 0$ and $f'(y(L_i)) = U_{yy}(L_i)$ in above approximation, we get,

$$f(y(L_i) + \epsilon_2) \approx U_{yy}(L_i)\epsilon_2$$

Therefore,

$$U_{yy}(L_i)\epsilon_2 + \frac{m_1}{(\epsilon_1 - \epsilon_2)^2} = 0$$

Which implies,

$$\boxed{U_{yy}(L_i)\epsilon_2 = -\frac{m_1}{(\epsilon_1 - \epsilon_2)^2}}$$

Let $\epsilon = \epsilon_1 - \epsilon_2$ be the separation between the two particles.

So,the derived equations using Taylor's approximation give ϵ_1 and ϵ_2 in the form,

$$\epsilon_1 = \frac{m_2}{U_{yy}(L_i)\epsilon^2}$$

$$\epsilon_2 = -\frac{m_1}{U_{yy}(L_i)\epsilon^2}$$

Using above values in $\epsilon = \epsilon_1 - \epsilon_2$ we get the following equation,

$$\epsilon = \frac{m_2}{U_{yy}(L_i)\epsilon^2} - \left(-\frac{m_1}{U_{yy}(L_i)\epsilon^2}\right)$$

$$\epsilon = \frac{m_2}{U_{yy}(L_i)\epsilon^2} + \frac{m_1}{U_{yy}(L_i)\epsilon^2}$$

$$\epsilon = \frac{m_1 + m_2}{U_{yy}(L_i)\epsilon^2}.$$

Multiplying both sides by ϵ^2 it becomes,

$$\epsilon^3 = \frac{m_1 + m_2}{U_{yy}(L_i)}$$

Taking the cube root gives,

$$\boxed{\epsilon = \left(\frac{m_1 + m_2}{U_{yy}(L_i)}\right)^{1/3}}$$

Now, we will put this value of ϵ to find ϵ_1 and ϵ_2 as follows,

For ϵ_1:

$$
\begin{aligned}
\epsilon_1 &= \frac{m_2}{U_{yy}(L_i)\epsilon^2} \\
\epsilon_1 &= \frac{m_2}{U_{yy}(L_i)\left[\left(\frac{m_1+m_2}{U_{yy}(L_i)}\right)^{1/3}\right]^2} \\
\epsilon_1 &= \frac{m_2}{U_{yy}(L_i)\left(\frac{m_1+m_2}{U_{yy}(L_i)}\right)^{2/3}} \\
\epsilon_1 &= \frac{m_2}{U_{yy}(L_i)^{1/3}(m_1+m_2)^{2/3}} \\
\epsilon_1 &= \frac{m_2}{[(m_1+m_2)^2 U_{yy}(L_i)]^{1/3}}
\end{aligned}
$$

For ϵ_2:

$$
\begin{aligned}
\epsilon_2 &= -\frac{m_1}{U_{yy}(L_i)\epsilon^2} \\
\epsilon_2 &= -\frac{m_1}{U_{yy}(L_i)\left(\frac{m_1+m_2}{U_{yy}(L_i)}\right)^{2/3}} \\
\epsilon_2 &= -\frac{m_1}{U_{yy}(L_i)^{1/3}(m_1+m_2)^{2/3}} \\
\epsilon_2 &= -\frac{m_1}{[(m_1+m_2)^2 U_{yy}(L_i)]^{1/3}}
\end{aligned}
$$

Therefore,

$$
\left.
\begin{aligned}
y_1 &= y(L_i) + \epsilon_1 = y(L_i) + \frac{m_2}{\left((m_1+m_2)^2\, U_{yy}(L_i)\right)^{1/3}} \\
y_2 &= y(L_i) + \epsilon_2 = y(L_i) - \frac{m_1}{\left((m_1+m_2)^2\, U_{yy}(L_i)\right)^{1/3}}
\end{aligned}
\right\} \tag{4.13}
$$

where $i = 1, 2, 3, 4$ and $y(L_i)$ is y-coordinate of L_i. Similarly, setting $y_1 = y_2 = 0$ in equations 4.7–4.10, equations 4.9 and 4.10 are identically satisfied, while the remaining equations become,

$$
x_1 - M\left(\frac{1}{x_1^2} + \frac{1}{(x_1-a)^2} + \frac{1}{(x_1+a)^2}\right) - \tilde{M}\left(\frac{2x_1}{(x_1^2+b^2)^{3/2}}\right) - \frac{m_2}{(x_1-x_2)^2} = 0, \tag{4.14}
$$

$$x_2 - M\left(\frac{1}{x_2^2} + \frac{1}{(x_2-a)^2} + \frac{1}{(x_2+a)^2}\right) - \tilde{M}\left(\frac{2x_2}{(x_2^2+b^2)^{3/2}}\right) + \frac{m_1}{(x_1-x_2)^2} = 0, \tag{4.15}$$

Their corresponding equilibrium solutions are,

$$\left.\begin{aligned} x_1 &= x(L_i) + \frac{m_2}{\left((m_1+m_2)^2\, U_{xx}(L_i)\right)^{1/3}} \\ x_2 &= x(L_i) - \frac{m_1}{\left((m_1+m_2)^2\, U_{xx}(L_i)\right)^{1/3}} \end{aligned}\right\} \tag{4.16}$$

where $i = 5, 6, 7, 8$ and $x(L_i)$ is the x-coordinate of L_i.

For the off-axis equilibrium points near L_9 , L_{10} and L_{12}, use the following equations ,

$$\left.\begin{aligned} x_1 &= x(L_i) + a_{11}\varepsilon_2 \\ x_2 &= x(L_i) + a_{21}\varepsilon_1 \\ y_1 &= y(L_i) + b_{11}\varepsilon_2 \\ y_2 &= y(L_i) + b_{21}\varepsilon_1 \end{aligned}\right\} \tag{4.17}$$

where $i = 9, 10, 11, 12$, and all the parameters are given as,

$$\begin{aligned} \varepsilon_j &= \frac{m_j}{(m_1+m_2)^{2/3}}, \qquad j = 1, 2, \\ a_{11} &= \frac{1}{\left(U_{xx}(L_i) + \frac{1}{\alpha_i}\, U_{xy}(L_i)\right)^{1/3}\left(1 + \frac{1}{\alpha_i}\right)^{1/2}}, \\ b_{11} &= -\frac{1}{\alpha_i}\, a_{11}, \\ \alpha_1 &= \beta + \gamma, \qquad \alpha_2 = \beta - \gamma, \\ \beta &= \frac{U_{yy}(L_i) - U_{xx}(L_i)}{2\, U_{xy}(L_i)}, \\ \gamma &= \left(\frac{(U_{xx}(L_i) - U_{yy}(L_i))^2 + 4(U_{xy}(L_i))^2}{4(U_{xy}(L_i))^2}\right)^{1/2}, \\ a_{21} &= -a_{11}, \qquad b_{21} = -b_{11}. \end{aligned}$$

4.3 Numerical Results

Throughout the calculation of the equilibrium points, using *Mathematica*, we set $m_1 = m_2 = 0.000001$.

4.3.1 Case 1 $(a = b = M = \tilde{M} = 1)$

In Case 1, we examine the equilibrium points of masses m_1 and m_2 for the parameters set $a = b = 1$ and $M = \tilde{M} = 1$ (see Table 4.1).

Table 4.1: Equilibrium points of the two test particles m_1 and m_2 for Case 1 $(a = b = M = \tilde{M} = 1)$.

Equilibrium points $L_i(x, y)$	$m_1(x_1, y_1)$	$m_2(x_2, y_2)$
$L_1(0,\ 0.51991)$	$(0,\ 0.52186)$	$(0,\ 0.51795)$
$L_2(0,\ -0.51991)$	$(0,\ -0.51795)$	$(0,\ -0.52186)$
$L_3(0,\ 1.92684)$	$(0,\ 1.93076)$	$(0,\ 1.92291)$
$L_4(0,\ -1.92684)$	$(0,\ -1.92291)$	$(0,\ -1.93076)$
$L_5(0.51991,\ 0)$	$(0.52186,\ 0)$	$(0.51795,\ 0)$
$L_6(-0.51991,\ 0)$	$(-0.51795,\ 0)$	$(-0.52186,\ 0)$
$L_7(1.92684,\ 0)$	$(1.93076,\ 0)$	$(1.92291,\ 0)$
$L_8(-1.92684,\ 0)$	$(-1.92291,\ 0)$	$(-1.93076,\ 0)$
$L_9(1.21443,\ 1.21443)$	$(1.21763,\ 1.21122)$	$(1.20939,\ 1.20939)$
$L_{10}(-1.21443,\ 1.21443)$	$(-1.20939,\ 1.20939)$	$(-1.21763,\ 1.21122)$
$L_{11}(1.21443,\ -1.21443)$	$(1.21946,\ -1.21946)$	$(1.21122,\ -1.21763)$
$L_{12}(-1.21443,\ -1.21443)$	$(-1.21122,\ -1.21763)$	$(-1.21946,\ -1.21946)$

4.3.2 Case 2 ($a = M = 1,\ b = 1.04232,\ \tilde{M} = 0.67$)

For these values, the equilibrium points of the test particles m_1 and m_2 are given in Table 4.2.

Table 4.2: Equilibrium points of the two test particles m_1 and m_2 for Case 2 ($a = M = 1$, $b = 1.04232$, $\tilde{M} = 0.67$).

Equilibrium points $L_i(x, y)$	$m_1(x_1, y_1)$	$m_2(x_2, y_2)$
$L_1(0,\ 0.59052)$	$(0,\ 0.59267)$	$(0,\ 0.58837)$
$L_2(0,\ -0.59052)$	$(0,\ -0.58837)$	$(0,\ -0.59267)$
$L_3(0,\ 1.83761)$	$(0,\ 1.84147)$	$(0,\ 1.83374)$
$L_4(0,\ -1.83761)$	$(0,\ -1.83374)$	$(0,\ -1.84147)$
$L_5(0.51137,\ 0)$	$(0.51332,\ 0)$	$(0.50941,\ 0)$
$L_6(-0.51137,\ 0)$	$(-0.50941,\ 0)$	$(-0.51332,\ 0)$
$L_7(1.89551,\ 0)$	$(1.89937,\ 0)$	$(1.89164,\ 0)$
$L_8(-1.89551,\ 0)$	$(-1.89164,\ 0)$	$(-1.89937,\ 0)$
$L_9(1.04556,\ 1.23821)$	$(1.04897,\ 1.23501)$	$(1.04082,\ 1.23313)$
$L_{10}(-1.04556,\ 1.23821)$	$(-1.04082,\ 1.23313)$	$(-1.04897,\ 1.23501)$
$L_{11}(1.04556,\ -1.23821)$	$(1.05030,\ -1.24328)$	$(1.04215,\ -1.24139)$
$L_{12}(-1.04556,\ -1.23821)$	$(-1.04215,\ -1.24139)$	$(-1.05030,\ -1.24328)$

4.3.3 Case 3 ($a = M = 1,\ b = 1.00367,\ \tilde{M} = 0.97$)

In this case, the results are shown in Table 4.3.

Table 4.3: Equilibrium points of the two test particles m_1 and m_2 for Case 3 ($a = M = 1$, $b = 1.00367$, $\tilde{M} = 0.97$).

Equilibrium points $L_i(x, y)$	$m_1(x_1, y_1)$	$m_2(x_2, y_2)$
$L_1(0,\ 0.52541)$	$(0,\ 0.52738)$	$(0,\ 0.52344)$
$L_2(0,\ -0.52541)$	$(0,\ -0.52344)$	$(0,\ -0.52738)$
$L_3(0,\ 1.91963)$	$(0,\ 1.92354)$	$(0,\ 1.91571)$
$L_4(0,\ -1.91963)$	$(0,\ -1.91571)$	$(0,\ -1.92354)$
$L_5(0.51907,\ 0)$	$(0.52103,\ 0)$	$(0.51712,\ 0)$
$L_6(-0.51907,\ 0)$	$(-0.51712,\ 0)$	$(-0.52103,\ 0)$
$L_7(1.92391,\ 0)$	$(1.92782,\ 0)$	$(1.91999,\ 0)$
$L_8(-1.92391,\ 0)$	$(-1.91999,\ 0)$	$(-1.92782,\ 0)$
$L_9(1.20045,\ 1.21691)$	$(1.20367,\ 1.21371)$	$(1.19543,\ 1.21185)$
$L_{10}(-1.20045,\ 1.21691)$	$(-1.19543,\ 1.21185)$	$(-1.20367,\ 1.21371)$
$L_{11}(1.20045,\ -1.21691)$	$(1.20546,\ -1.22196)$	$(1.19722,\ -1.22010)$
$L_{12}(-1.20045,\ -1.21691)$	$(-1.19722,\ -1.22010)$	$(-1.20546,\ -1.22196)$

4.4 Physical Interpretation and Symmetry of the Equilibrium Solutions

Twelve equilibrium points $L_i(x, y)$ given in table 3.1 serve as the foundation for finding the location of two test particles m_1 and m_2. These are the positions of secondary bodies where all the forces of primaries become equal and if any test particle or particles come here will become stationary with respect to the primaries. The point (x_1, y_1) is the position of first test particle m_1 and it experiences an extra force from m_2 so m_1 shifts away from $L_i(x, y)$. Likewise, (x_2, y_2) is the position of the second test particle, which experiences an extra force from m_1 and shifts opposite to m_1 relative to $L_i(x, y)$.

When the mutual gravitational interaction between the two small masses m_1 and m_2 is taken into account, the single equilibrium point $L_i(x, y)$ bifurcates into two distinct equilibrium positions, denoted by $m_1(x_1, y_1)$ and $m_2(x_2, y_2)$. Physically, two small masses cannot occupy the same location. Consequently, instead of both masses residing at the equilibrium point $L_i(x, y)$, they form a co-orbital pair positioned symmetrically about the point L_i. Thus, the equilibrium solutions of two secondary msses are small perturbations of the equilibrium points L_i .

The 12 equilibria arise from the symmetry of the rhomboidal CC. The four axial points L_1–L_4 on the $y-$axis—exist because the gravitational pull from the primaries $(0, \pm b)$ can balance the centrifugal force along the vertical axis. The four collinear points L_5–L_8 on the x-axis are a direct generalization of the Euler collinear points L_1, L_2, L_3 of the CR3BP, with an additional point appearing due to the presence of the central primary body. The four non-collinear points L_9–L_{12} are analogous to the triangular Lagrange points L_4, L_5, where the combined gravity from the five primaries creates isolated regions along the axes.

The rhomboidal CC of the five primaries possesses D_{2h} symmetry, being invariant under reflections about both coordinate axes and a rotation of $180°$ about the origin. This symmetry reduces the computational effort. When the mutual interaction between m_1 and m_2 is included, the D_{2h} symmetry is preserved, provided both test particles are transformed simultaneously. The mutual gravity of test particles pull m_1 and m_2 towards each other so their positions must be symmetric about the original point $L_i(x, y)$, displaced towards each others to remain at equilibrium. For instance, in Table 4.3, when $x = 0.51907$, then $x_1 = 0.52103$ (shift $+0.00196$) and $x_2 = 0.51712$ (shift -0.00195); and when $y = 1.91963$, then $y_1 = 1.92354$ (shift $+0.00391$) and $y_2 = 1.91571$ (shift -0.00392).

The left-right mirror of the rhombus gives the left-right mirror of the equilibrium: the gravity from the primary at $(+a, 0)$ swaps with that from the primary at $(-a, 0)$. Similarly, the top-bottom mirror of the rhombus gives the top-bottom mirror of the equilibrium. The non-collinear equilibria L_9–L_{12} lie off both coordinate axes and satisfy the exact symmetry relations

$$\begin{aligned} x(L_{10}) &= -x(L_9), & y(L_{10}) &= y(L_9), \\ x(L_{11}) &= x(L_9), & y(L_{11}) &= -y(L_9), \\ x(L_{12}) &= -x(L_9), & y(L_{12}) &= -y(L_9). \end{aligned}$$

4.5 Linear Stability Analysis

To examine the stability of the equilibrium points, we applied the classical linearization technique. The necessary and sufficient criteria for stability are established using the Routh–Hurwitz criterion [36]. We linearize the equations of motion for the test particle in the neighborhood of each equilibrium point. Let (x, y) denotes the coordinates of an equilibrium point in the dynamical system, and suppose that the test particle undergoes a small perturbation (x_0, y_0). Consequently, the perturbed position of the particle is represented by $(x + x_0,\ y + y_0)$.

Expanding U_x and U_y in a first-order Taylor series about the equilibrium point and substituting the resulting expressions into the equations of motion gives

$$\begin{aligned} \ddot{x}_0 - 2\dot{y}_0 &= x_0 U_{xx}(L_i) + y_0 U_{xy}(L_i), \\ \ddot{y}_0 + 2\dot{x}_0 &= x_0 U_{yx}(L_i) + y_0 U_{yy}(L_i), \end{aligned} \tag{4.18}$$

Note that $U_{yx} = U_{xy}$, because the mixed partial derivatives commute.

Because these are linear differential equations with constant coefficients, we assumethe solutions of the form,

$$x_0(t) = C_1 e^{\lambda t}, \qquad y_0(t) = C_2 e^{\lambda t}.$$

Then,

$$\dot{x}_0 = \lambda C_1 e^{\lambda t}, \qquad \dot{y}_0 = \lambda C_2 e^{\lambda t},$$

$$\ddot{x}_0 = \lambda^2 C_1 e^{\lambda t}, \qquad \ddot{y}_0 = \lambda^2 C_2 e^{\lambda t}.$$

using these in equation 4.18 we have ,

$$(\lambda^2 - U_{xx}(L_i))\, C_1 + (-2\lambda - U_{xy}(L_i))\, C_2 = 0,$$
$$(2\lambda - U_{xy}(L_i))\, C_1 + (\lambda^2 - U_{yy}(L_i))\, C_2 = 0.$$

The above system is a homogeneous system of equations in C_1 and C_2. For the non-trivial solution of this system,

$$\begin{vmatrix} \lambda^2 - U_{xx}(L_i) & -2\lambda - U_{xy}(L_i) \\ 2\lambda - U_{xy}(L_i) & \lambda^2 - U_{yy}(L_i) \end{vmatrix} = 0.$$

Expanding this determinant gives exactly

$$\lambda^4 + (4 - U_{xx}(L_i) - U_{yy}(L_i))\, \lambda^2 + \big(U_{xx}(L_i) U_{yy}(L_i) - U_{xy}^2(L_i)\big) = 0. \tag{4.19}$$

So the characteristic polynomial in λ is,

$$\lambda^4 + A\lambda^2 + B = 0, \tag{4.20}$$

where $A = 4 - U_{xx}(L_i) - U_{yy}(L_i)$ and $B = U_{xx}(L_i)U_{yy}(L_i) - U_{xy}^2(L_i)$.

An equilibrium point is linearly stable under a small perturbation if all four roots of λ of characteristic equation 4.20 are purely imaginary. Now, setting $\lambda^2 = z$, we have,

$$z^2 + Az + B = 0. \tag{4.21}$$

the two roots of equation 4.21,

$$z = \frac{-A \pm \sqrt{A^2 - 4B}}{2},$$

must be real and negative. The results are shown in the following tables for all three cases.

Table 4.4: (Case 1)Eigenvalues for the stability analysis of the equilibrium points.

Equilibrium points $L_i(x, y)$	**Eigenvalues** λ	**Stability**
$L_{1,2}\,(0,\ \pm 0.51991)$	$\pm 5.53145,\ \pm 3.84218i$	Unstable
$L_{3,4}\,(0,\ \pm 1.92684)$	$\pm 1.12927,\ \pm 1.28223i$	Unstable
$L_{5,6}\,(\pm 0.51991,\ 0)$	$\pm 5.53145,\ \pm 3.84218i$	Unstable
$L_{7,8}\,(\pm 1.92684,\ 0)$	$\pm 1.12927,\ \pm 1.28223i$	Unstable
$L_{9,10,11,12}\,(\pm 1.21443,\ \pm 1.21443)$	$\mp 0.728216 \pm 0.924513i$	Unstable

Table 4.5: (Case 2)Eigenvalues for the stability analysis of the equilibrium points.

Equilibrium points $L_i(x, y)$	**Eigenvalues** λ	**Stability**
$L_{1,2}\,(0,\ \pm 0.59052)$	$\pm 4.74034,\ \pm 3.30437i$	Unstable
$L_{3,4}\,(0,\ \pm 1.83761)$	$\pm 1.21376,\ \pm 1.31666i$	Unstable
$L_{5,6}\,(\pm 0.51137,\ 0)$	$\pm 5.53033,\ \pm 3.92287i$	Unstable
$L_{7,8}\,(\pm 1.89551,\ 0)$	$\pm 1.22587,\ \pm 1.33786i$	Unstable
$L_{9,10,11,12}\,(\pm 1.04556,\ \pm 1.23821)$	$\mp 0.776116 \pm 0.941243i$	Unstable

Table 4.6: (Case 3)Eigenvalues for the stability analysis of the equilibrium points
.

Equilibrium points $L_i(x,y)$	**Eigenvalues** λ	**Stability**
$L_{1,2}\,(0,\ \pm 0.52541)$	$\pm 5.4593,\ \pm 3.79257i$	Unstable
$L_{3,4}\,(0,\ \pm 1.91963)$	$\pm 1.13625,\ \pm 1.28507i$	Unstable
$L_{5,6}\,(\pm 0.51907,\ 0)$	$\pm 5.53062,\ \pm 3.84937i$	Unstable
$L_{7,8}\,(\pm 1.92391,\ 0)$	$\pm 1.13799,\ \pm 1.28715i$	Unstable
$L_{9,10,11,12}\,(\pm 1.20045,\ \pm 1.21691)$	$\mp 0.73264 \pm 0.917021i$	Unstable

The numerical evaluation of the eigenvalues for all equilibrium points for tested parameters indicates the unstability in the ranges considered. On the basis of this analysis, we can say that our 24 equilibrium points for the two infinitesimal masses are unstable, because $L_i(x,y)$, where $i = 1,2,3,\ldots,12$, acts as the center of mass for the positions of $m_1(x_1,y_1)$ and $m_2(x_2,y_2)$.

Instability implies that the test particles placed at exact equilibrium points will not remain there under small perturbations.

4.6 Zero-Velocity Curves and Hill Regions

We define the effective potential as:

$$\begin{aligned} U(x,y) = \frac{1}{2}(x^2+y^2) + M\left(\frac{1}{|r_0-r_1|} + \frac{1}{|r_0-r_2|} + \frac{1}{|r_0-r_3|}\right) \\ - \tilde{M}\left(\frac{1}{|r_0-r_4|} + \frac{1}{|r_0-r_5|}\right), \end{aligned} \tag{4.22}$$

where all the distances are defined in equations 3.15.

The Jacobian integral is given by Curtis [32] is,

$$2U + C = v^2, \tag{4.23}$$

where v^2 is speed squared of an infinitesimal mass in the rotating coordinate system is defined as,

$$v^2 = \dot{x}^2 + \dot{y}^2, \tag{4.24}$$

Since v^2 cannot be negative so,

$$2U + C \geq 0. \tag{4.25}$$

This equation indicates the allowed region of motion for both secondary masses because ($m_1 = m_2 = 10^{-6}$) is just a small perturbation to the case of single test mass. The boundary separating the permissible and forbidden regions of motion is obtained by putting $v = 0$, i.e,

$$2U + C = 0\ , \tag{4.26}$$

$$U = -\frac{C}{2}\ . \tag{4.27}$$

These ZVCs divide the plane into allowed and forbidden regions of motion for a given Jacobi constant C. The geometry of zero-velocity curves changes as the mass and distance parameters and jacobi constant vary. They play a fundamental role in accessibility of equilibrium points.

Figure 4.2 shows the ZVCs for two different rhombus configurations with fixed a and as b changes, the shape and connectivity of these curves also change.The white circles mark the locations of the five primaries, one at the origin and four at $(\pm 1, 0)$ and $(0, \pm b)$. The blue shaded regions are energetically forbidden while the brown and orange regions are allowed for motion.

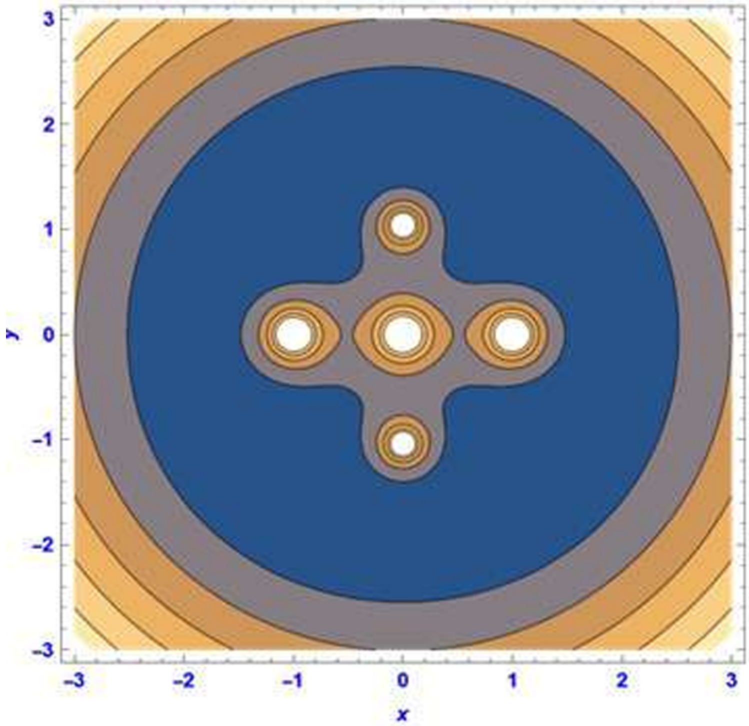

(a)

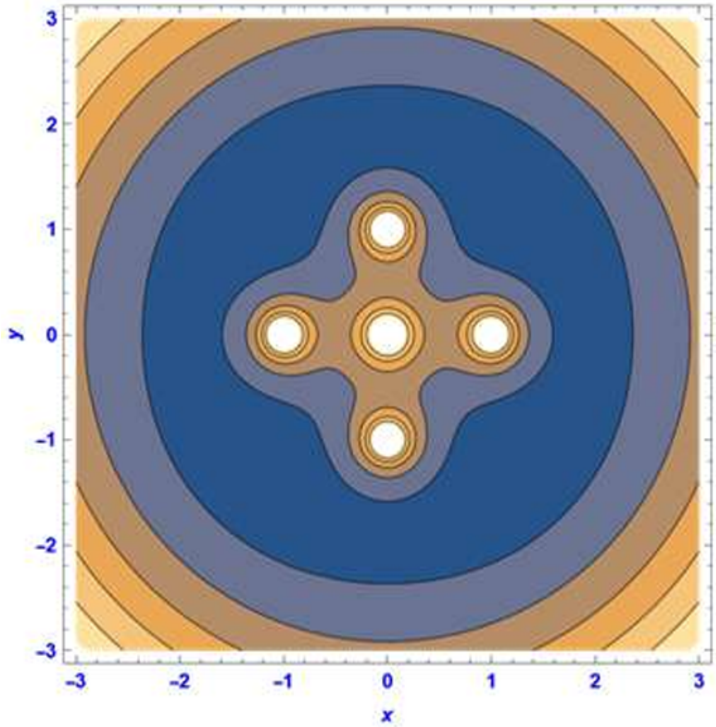

(b)

Figure 4.2: Evolution of ZVCs: (a) $a = \tilde{M} = 1$, $b = 1.04232$, $\beta = 0.67$; (b) $a = \tilde{M} = 1$, $b = 1.00367$, $M = 0.97$.

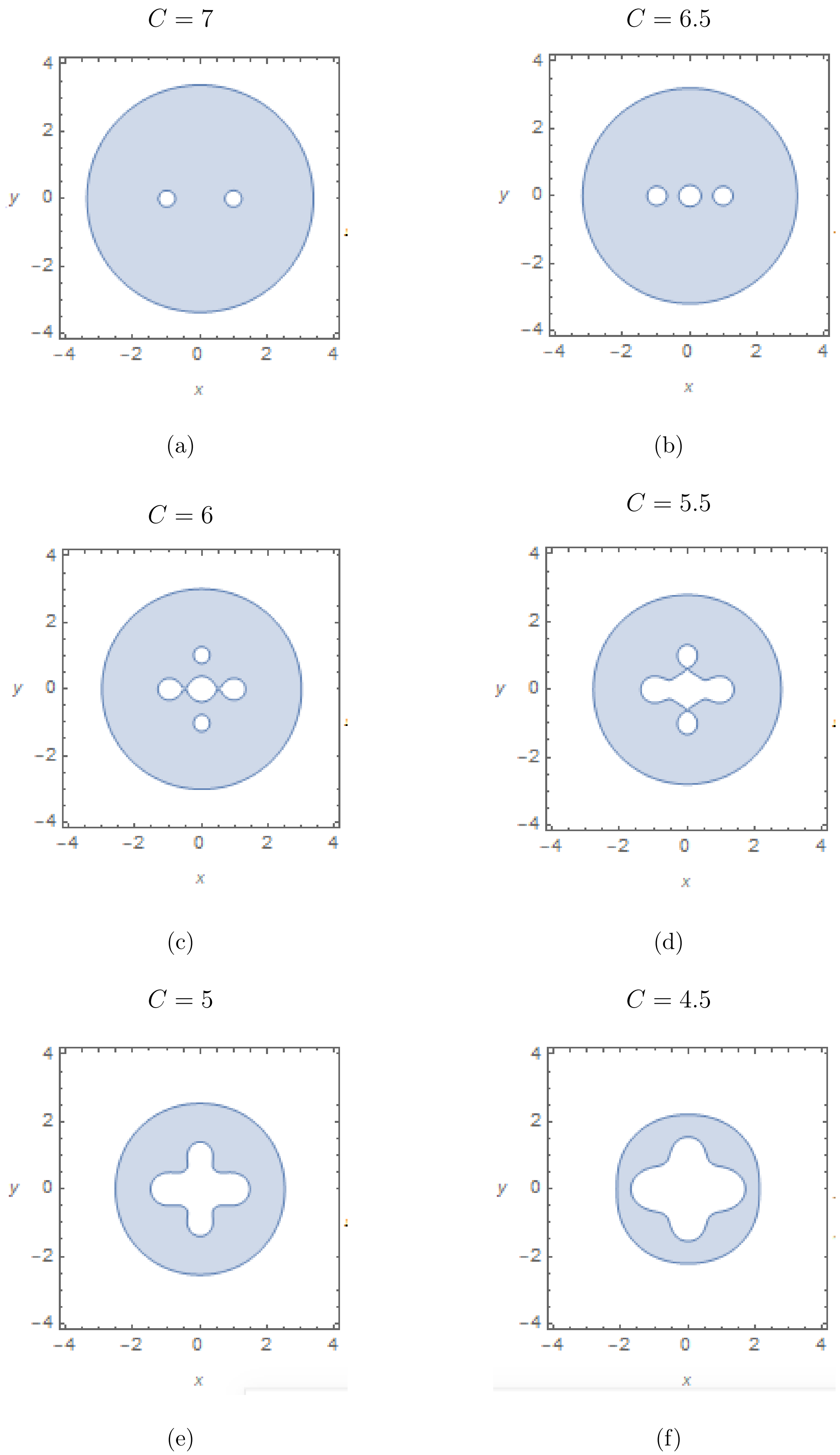

Figure 4.3: The possible regions of motion for infinitesimal masses (white regions) when $a = M = 1$, $b = 1.04232$, $\tilde{M} = 0.67$ for energy interval $C \in (7, 4.5)$.

Figure 4.3 illustrate the possible regions of motion for two secondary bodies in the central configuration of primaries for different energy intervals.

When the value of C is very high (i.e., C=7), it implies the low energy, so the forbidden shaded region is very thick. In this case, only the two outermost primaries lying at the x-axis are energetically accessible. For C=6.5, we see the gray disk with three collinear white holes at x-axis.

Now the three primaries at the x-axis are accessible, but there is no access to y-axis masses. When C=6, then all the five primaries lie in the U $<$ C region, but the necks between them are still closed. For C=5.5, the five holes start connecting. The ZVCs pinch and open now. The bridges between all the primaries widen into a clear '+' shape for C=5. The forbidden region now has just 4 lobes in the quadrants. For very low values of Jacobi constant (i.e.C=4.5) the energy becomes high and the forbidden region is a thin ring. Now the test particles can go almost anywhere, except near the diagonal directions where U is still greater than C.

For the same energy interval of C, the accessible regions of motion for infinitesimal masses m_1 and m_2 for the case when $a = M = 1$, $b = 1.00367$, $\tilde{M} = 0.97$ are given in Figure 4.4. The five white dots are showing the positions of five primary masses. For the high energy C=7, the gray region is a big disk and there are five ting islands exist around each primary body. The particle is trapped and cannot move among the massive primaries. For C=6.5, the five allowed regions become bit bigger but still there is no connection between them. Bt when the value of jacobi constant decreases to 6, the center and four outer primary bodies connected into a plus + shape. For the value 5.5, the shape of + gets thicker and the forbidden gray region gets thinner therefore become more accessible. For C=5, the gray ring is even thinner and the allowed white region is almost whole box. Finally corresponding to the lowest value of C, the allowed white region connects all the primary bodies and the infinitesimal particles can now travel between them. These regions of motions are not just math plots.They are used in real astrodynamics to understand where the spacecrafts or asteroids can travel in the rhomboidal five-body system for the given energy level.

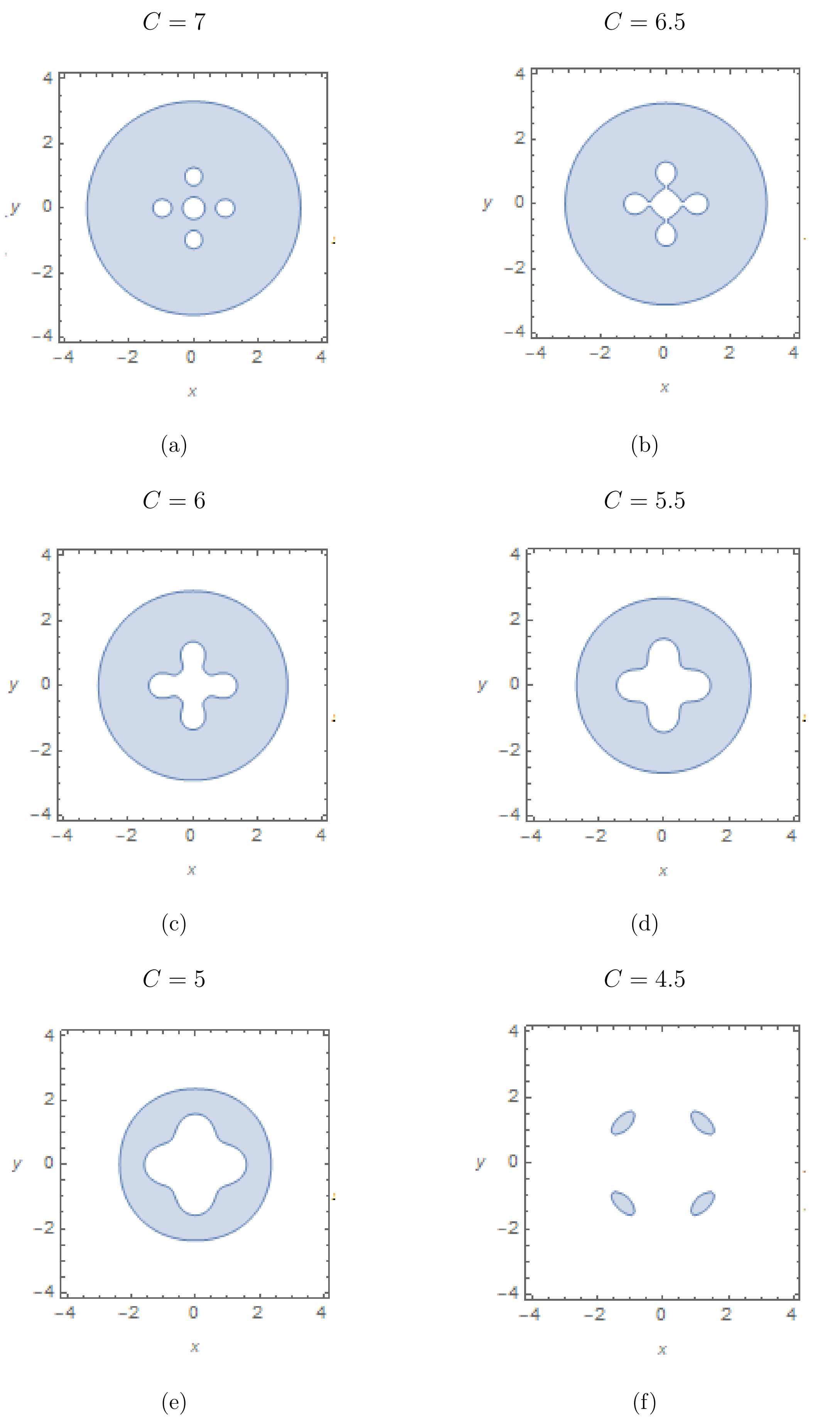

Figure 4.4: The allowed regions of motion for infinitesimal masses (white regions) when $a = M = 1$, $b = 1.00367$, $\tilde{M} = 0.97$ for energy interval $C \in (7, 4.5)$.

Chapter 5

Conclusion

In this thesis, we have extended the restricted rhomboidal six-body problem by including one more secondary body and considering the mutual gravitational interaction between two infinitesimal masses m_1 and m_2. Two test particles are placed under the gravitational influence of five primaries forming a planar rhombus. Firstly, by using the condition of central configuration we derived the mass ratio function in terms of shape parameters a and b for five primary bodies with masses $M_1 = M_2 = M_3 = M$ and $M_4 = M_5 = \tilde{M}$ and also found its interval of continuity and discussed some particular cases in that interval.

Next, the equations of motion for both secondary bodies are modeled in a rotating reference fame for equilibrium solutions, resulting a coupled nonlinear algebraic system of equations 4.7–4.10. We recovered twelve equilibrium points for RR6BP (4 lie at the x-axis, 4 at the y-axis and 4 located off-axes) and linearized the equations about those points by following Whipple's perturbation approach to find the location of equilibrium points for two secondary bodies. From the results, it is concluded that when the mutual gravitational interaction between two test particles is taken into account with $m_1 = m_2 = 10^{-6}$, each equilibrium point presented in table 3.1 bifurcates into a symmetric pair. The center of mass of each symmetric pair aligns with the position of the corresponding unperturbed equilibrium point.

Furthermore, the symmetry of the rhomboidal CC is reflected in the numerical results. So, only three independent points for each case need to be calculated, the remaining nine following by symmetry. As the mass and distance parameters are varied, the equilibrium points also change their positions relative to the primaries but the total count of equilibrium points remained same. Finally, we analyzed the stability of solutions and found that all the equilibrium points are linearly unstable. We also studied the evolution of zero-velocity curves for fixed values of masses and presented the accessible regions of motion for infinitesimal masses. We also identified the value of the Jacobian constant C for different energy intervals. The results are relevant to co-orbital binary asteroids and moons, spacecraft formation flying at Lagrange points, and the search for Trojan, exoplanets etc. Although unstable, they can provide temporary trapping regions for dust and small bodies over several orbital periods.

Bibliography

[1] Isaac Newton. *"Philosophiae Naturalis Principia Mathematica"*, volume 2000. University of California Digital Library, 2000.

[2] J. L. Russell. "kepler's laws of planetary motion: 1609–1666". *The British Journal for the History of Science*, 2(1):1–24, 1964.

[3] A. Wintner. *"The Analytical Foundations of Celestial Mechanics"*. Courier Corporation, 2014.

[4] J. F. L Simmons, A. J. C McDonald, and J. C. Brown. "the restricted 3-body problem with radiation pressure". *Celestial Mechanics*, 35(2):145–187, 1985.

[5] S. R. Bistafa. "euler's three-body problem". *Euleriana*, 1(2):181–187, 2021.

[6] F. J. T. Salazar, A.J. Rosales, and J.L. Flores, M.R.and Santos. "three-body problem, its lagrangian points and how to exploit them using an alternative transfer to l4 and l5". *Celestial Mechanics and Dynamical Astronomy*, 114(1-2):201–213, 2012.

[7] J. Barrow-Green. *"Poincaré and the Three Body Problem"*, volume 11. American Mathematical Society, 1997.

[8] V. Szebehely and E. Grebenikov. "theory of orbits–the restricted problem of three bodies". *Soviet Astronomy*, 13:364, 1969.

[9] A. L. Whipple. "equilibrium solutions of the restricted problem of 2+2 bodies". *Celestial Mechanics*, 33(3):271–294, 1984.

[10] F. R. Moulton. "on a class of particular solutions of the problem of four bodies". *Transactions of the American Mathematical Society*, 1(1):17–29, 1900.

[11] M. Kulesza, M. Marchesin, and C. Vidal. "restricted rhomboidal five-body problem". *Journal of Physics A: Mathematical and Theoretical*, 44(48):485204, 2011.

[12] A. Albouy and V. Kaloshin. "finiteness of central configurations of five bodies in the plane". *Annals of Mathematics*, pages 535–588, 2012.

[13] A. Ollongren. "on a restricted five-body problem: An analysis with computer algebra". In *The Few Body Problem: Proceedings of the 96th Colloquium of the International Astronomical Union Held in Turku, Finland, June 14–19, 1987*, Dordrecht, 1988. Springer Netherlands.

[14] K. E. Papadakis and S. S. Kanavos. "numerical exploration of the photogravitational restricted five-body problem". *Astrophysics and Space Science*, 310(1):119–130, 2007.

[15] M. Gidea and J. Llibre. "symmetric planar central configurations of five bodies: Euler plus two". *Celestial Mechanics and Dynamical Astronomy*, 106(1):89, 2010.

[16] T. Lee and M. Santoprete. "central configurations of the five-body problem with equal masses". *Celestial Mechanics and Dynamical Astronomy*, 104(4):369–381, 2009.

[17] J. I. Palmore. "relative equilibria of vortices in two dimensions". *Proceedings of the National Academy of Sciences*, 79(2):716–718, 1982.

[18] M. Shoaib, A. R. Kashif, and I. Szücs-Csillik. "on the planar central configurations of rhomboidal and triangular four- and five-body problems". *Astrophysics and Space Science*, 362(10):182, 2017.

[19] J. Singh and A. E. Vincent. "equilibrium points in the restricted four-body problem with radiation pressure". *Few-Body Systems*, 57(1):83–91, 2016.

[20] M. Corbera, J. M. Cors, and G. E. Roberts. "classifying four-body convex central configurations". *arXiv preprint arXiv:1903.01684*, 2019.

[21] R. Lara and A. Bengochea. "a restricted four-body problem for the eight figure choreography". *arXiv preprint arXiv:1910.12822*, 2019.

[22] A. Alsaedi, F. Yousaf, S. Bushnaq, and S. Momani. "new styles of periodic solutions of the classical six-body problem". *Mathematics and Computers in Simulation*, 159:183–196, 2019.

[23] M. J. Idrisi and M. Shahbaz Ullah. "central-body square configuration of restricted six-body problem". *New Astronomy*, 79:101381, 2020.

[24] E. E. Zotos. "exploring the location and linear stability of the equilibrium points in the equilateral restricted four-body problem". *International Journal of Bifurcation and Chaos*, 30(10):2050155, 2020.

[25] E. E. Zotos. "basins of convergence of equilibrium points in the pseudo-newtonian planar circular restricted three-body problem". *Astrophysics and Space Science*, 362(10):195, 2017.

[26] M. A. R. Siddique, A.R. Kashif, M. Shoaib, and S. Hussain. "stability analysis of the rhomboidal restricted six-body problem". *Advances in Astronomy*, 2021(1):5575826, 2021.

[27] M. R. Spiegel. *"Theory and Problems of Theoretical Mechanics (Schaum's Outline)"*. McGraw-Hill, 2021.

[28] D. B. Meli. "the relativization of centrifugal force". *Isis*, 81(1):23–43, 1990.

[29] V. Szebehely and R. Broucke. "determination of the potential in a synodic system". *Celestial Mechanics*, 24(1):23–26, 1981.

[30] W. H. Goodyear. "completely general closed-form solution for coordinates and partial derivative of the two-body problem". *Astronomical Journal, Vol. 70, p. 189*, 70:189, 1965.

[31] K. R. Meyer. *"Periodic Solutions of the N-Body Problem"*, volume 1719. Springer Science & Business Media, 1999.

[32] H. D. Curtis. *"Orbital Mechanics for Engineering Students"*. Butterworth-Heinemann, third edition, 2014.

[33] Wen-tsun Wu. "on wintner's conjecture about central configurations". In *International Workshop on Mathematics Mechanization*, Berlin, Heidelberg, 2004. Springer Berlin Heidelberg.

[34] K. Chang and K. Chen. "rhomboidal central configurations of the five-body problem". *Regular and Chaotic Dynamics*, 31(3):468–483, 2026.

[35] P. Ramond. "the abel–ruffini theorem: Complex but not complicated". *The American Mathematical Monthly*, 129(3):231–245, 2022.

[36] E. X. DeJesus and C. Kaufman. "routh-hurwitz criterion in the examination of eigenvalues of a system of nonlinear ordinary differential equations". *Physical Review A*, 35(12):5288, 1987.